


Article

Mineralogy and Geochemistry of Fluvial-Lacustrine Pisolith Micronodules from the Roztoka Odrzańska, Odra River, NW Poland

Łukasz Maciąg ^{1,*} , Urszula Rydzewska ², Artur Skowronek ² and Sylwester Salwa ³

¹ Institute of Marine and Environmental Sciences, University of Szczecin, Adama Mickiewicza 18, 70-383 Szczecin, Poland

² Polish Geological Institute—National Research Institute, Pomeranian Branch, Wieniawskiego 20, 71-130 Szczecin, Poland; urszula.rydzewska@pgi.gov.pl (U.R.); artur.skowronek@pgi.gov.pl (A.S.)

³ Polish Geological Institute—National Research Institute, Holy Cross Mts. Branch, Zgoda 21, 25-953 Kielce, Poland; sylwester.salwa@pgi.gov.pl

* Correspondence: lukasz.maciag@usz.edu.pl; Tel.: +48-91-444-23-71

Received: 17 November 2019; Accepted: 17 December 2019; Published: 20 December 2019



Abstract: Small-sized ferruginous micronodules or pisolith nodules, frequently occurring in inland freshwater systems in moderate climate zones, are important indicators of groundwater level changes and early diagenetic processes, especially within the Pleistocene post-glacial sedimentary systems, including swamps, peatbogs, rivers, or lakes. Compared to the other geochemical environments, pisolith nodules are usually dominated by iron hydroxides and oxides. In most cases, described micronodules indicate high phosphatization, significant contribution of allochthonous detrital components, and low manganese content. The major aim of the article is to present textural, geochemical, and mineralogical variability of pisolith nodules recovered from the Roztoka Odrzańska, Odra river mouth area, NW Poland. We describe genetical relations between different types of pisoliths and try to interpret the possible formation phenomena. Analyzed loose ferruginous micronodules were separated from the lacustrine silty-clayey sapropel muds and gyttja, later analyzed using optical microscopy, SEM-energy dispersive x-ray (EDX), and XRD methods. As a reference material, we use archival iron bog ores and geochemical data of different types of nodules. Additionally, we describe previously unknown siderite-rich nodules found in neighboring sites of the Dąbie Lake and the Szczecin Lagoon.

Keywords: micronodules; nodules; pisolith; ferruginous micronodules; lacustrine sediments; sapropel; gyttja; peat; Quaternary; iron bog

1. Introduction

Different kinds of nodules and micronodules are important components of rocks and sediments, being extensively found in all sedimentary environments, such as deep-sea basins [1] or terrestrial ferromanganese deposits [2,3]. Loose nodules and micronodules from the recent Quaternary lacustrine-fluvial environments are less frequent. Due to the weak economic potential and low contents of strategic metals, ferruginous pisoliths are not described very often in the literature [4–6]. Compared with the oceanic ferromanganese nodules, the lake, lacustrine, or river formed nodules and micronodules do not indicate increased contents of cobalt, nickel, copper, or rare earth elements. Considering the differences of trace element concentration and growth (nucleation) rate, the lacustrine nodules form much faster than oceanic polymetallic nodules, however in some cases do not significantly differ in shape, texture, or general chemical composition from the Fe-rich micronodules or nodules from oceanic basins [7].

The formation and occurrence of pisoliths in the young Quaternary sedimentary environments is a relatively puzzling and complex issue, being a subject of numerous mineralogical and geochemical studies [2,6,8–12].

The pisolith nodules and micronodules found in recent lacustrine-fluvial sediments, solid rocks, or soils are usually dominated by iron and called “iron bog ores” [13]. These kinds are usually associated with swamps, peats, and lacustrine sediments, being also classified as oxidized and reduced types [14,15]. The iron bog ores are also divided into fine ores (or “soft”), represented by loose deposits, and cemented ores (lump or “hard”), resembling slags and ferruginous sandstones or mudstones. Iron bog ores and associated Fe-rich or carbonate nodules are formed in the river valleys and lowlands, where the groundwater level is elevated [16].

Bog ores occur in three macro-morphological forms of decreasing size: (i) as a continuous, horizontal and cemented layer; (ii) as the randomly distributed ore blocks forming horizons, usually of 1 cm or more in diameter; (iii) loose ferruginous horizontal concentrations, mostly below 10 mm in diameter [13]. Additionally, the ferruginous material shows great micro-morphological variability, being found as pisoliths and continuous crusts (ferricretes or laterites), corresponding to ferric, plinthic, petroplinthic, and pisoplinthic horizons [17].

The pisoliths (also called pisoids or coniatolites) are formed as micronodules—spherical or ellipsoidal grains of concentric texture and a typical diameter of 2–10 mm, classified in a group of ooclasts (>2 mm in diameter) or ooids (<2 mm). Pisoliths consist of a nucleus, one or more concentric layers and an outer casing (cortex). The growth of the cortex is continuous and occurs at the expense of dissolving and remobilizing the material from the nucleus, even to full replacement with new minerals. The outer layer is often characterized by greater hydration. The dominant processes are rehydration and, secondary, crystallization. In the terrestrial conditions, the mineral composition is dominated by hematite and goethite. Iron minerals often exhibit structural enrichment and incorporation into clays [18,19].

The pisoliths form as a result of (i) chemical precipitation in turbulent water or the terrestrial environment; (ii) chemical and biochemical precipitation from calm water; (iii) early-diagenetic processes, especially in tropical and subtropical climates. The type (i) is evenly shaped, circular or ellipsoidal, and indicates flat external surfaces. Type (ii) often does not indicate a detritic nucleus and shows an irregular or concentric internal structure (type iii). Pisoliths usually do not indicate any organic structures [20], however, they may show bio- and geochemical origins and occur in rocks and sediments formed in various climate zones, from humid tropical climates to cool and dry polar climates [21]. Bio-processes may include biogenic dispersion of metals, biogeochemical precipitation in soils, especially within zones of plants activity, microbial processes, greater admixtures of siliceous material, such as diatoms, or influx of fertilizers rich in P and S. Geochemical processes are related mostly to climate zonation, variability, or redox conditions (dissolution and reprecipitation) and acquisition of Fe, Mn, Al, and Si. Pisolith nodules may not display a detrital solid nucleus, such as quartz, and arise as a result of epigenetic processes, associated with the transformation of clay minerals [22].

Anand and Paine [23] classify iron and aluminum-rich pisoliths into four groups: (i) homogeneous, with no visible internal structure; (ii) lithorific, which shows a solid clavicle and a thin external mineral layer; (iii) pseudomorphic, in which all minerals are secondary, however, the original internal structure is still noticeable; (iv) concentric, consisting of a series of concentric layers. The individual types may indicate a number of fine admixtures of detrital or less soluble material.

According to the mineralogical classification of pisoliths, few types are distinguished: (i) carbonate (dominated by calcite, aragonite, siderite or rhodochrosite), (ii) bauxite, (iii) gibbsite, (iv) hematite, (v) goethite, (vi) chamosite, (vii) siliceous and (viii) phosphate. All types are found also in mixed compositions [24].

The mineral composition of pisolith micronodules is dominated by authigenic Fe-(Mn) oxides and oxyhydroxides (hematite, goethite, maghemite, ferrihydrite, feroxyhyte, wüstite, and rare native

iron), as well as aluminum minerals (boehmite, gibbsite, hydrargillite, anatase), phosphates, sulphates, carbonates, clays, and allogenic detrital minerals (quartz, feldspars, zircon). The manganese minerals are scarce [8,25–28]. Several nodules and micronodules contain a solid detrital core and extensive Fe-(Mn) lamination [29], however, in some cases may be carbonate-rich [30]. Some pisoliths have internal cracks and veins, sometimes of a concentric nature. In extreme cases, as a result of the total discharge of mineral material from the nucleus, voids are especially noticeable [2].

Formation of Fe-rich precipitates is often associated with soil processes, such as bioaccumulation, the formation of weathering or illuvium horizons, adsorption on clay/organic particles or root exudation [22]. Some pisoliths are known also from pre-quaternary solid rocks and old soil horizons [11,16,17,27]. Nahon [22] describes pisoliths (pisolith concretions) as a result of the “glaebulisation” processes. The glaebulisation is a phenomenon of local dissolution of primary components and in situ crystallization of new minerals, mainly due to the iron remobilization and dilution. The final product of these processes are cracks and fissures as septarian shapes [31].

2. Study Area

The Róztoka Odrzańska is a small intermixing water basin of the Odra river mouth and Szczecin Lagoon, located around 20 km north from the city of Szczecin, NW Poland (Figure 1). It covers the area of 26.3 km², has a length of 9 km, a width of 1.1 km in the southern part (up to 5.7 km in the central part) and an average depth of 3.5 m. The middle part of the Róztoka Odrzańska is cross-cut by the artificially created fairway of approximately 12 m of depth [32].

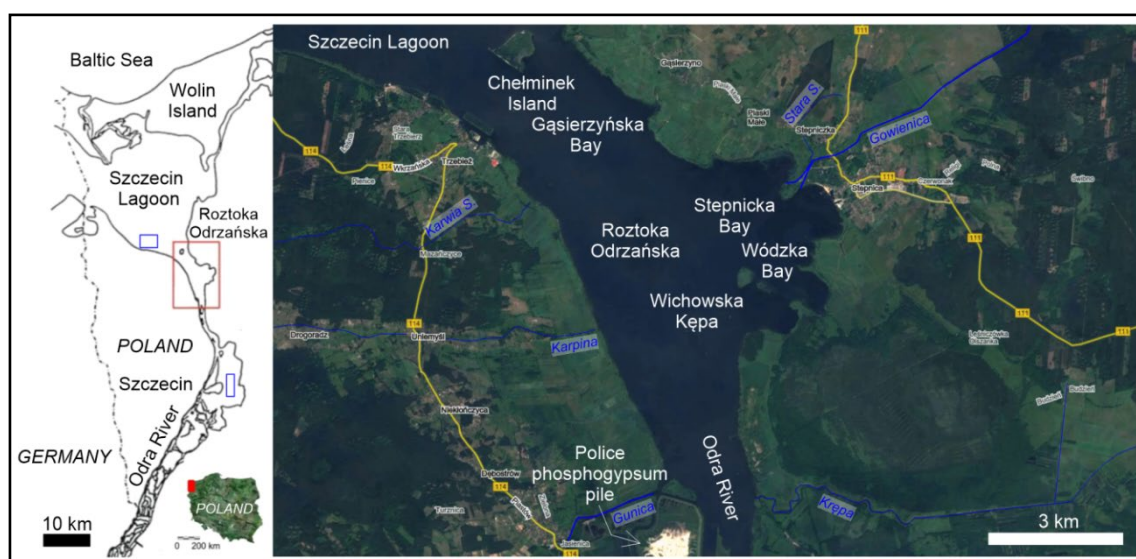


Figure 1. Location of the study area. The Róztoka Odrzańska is marked by a red rectangle; blue rectangles show sampling stations on the Dąbie Lake and the Szczecin Lagoon, where previously non-described reference material was collected ([32,33]; slightly modified).

The area of investigation is a subject of complex hydrological processes, such as (i) exchange and intermixing of sea with freshwater, where the marine inflow can reach even up to 100 km inland; (ii) a complicated river channel system, with dense net of irrigation canals; (iii) significant water level changes, related mainly to windy storms and baric wave surges of the Baltic Sea [32,34].

The Róztoka Odrzańska is strongly affected by anthropogenic impacts, mainly related to industrial and agricultural contamination of surface water and sediments by heavy metals and biogenic compounds. Several anthropogenic forms in the area adjacent to the Róztoka Odrzańska are distinctive, including flood embankments, water dikes, and irrigating canals. On the west bank of the Odra River, the large pile of phosphogypsum, with a height of about 20 m was created through the industrial

activity of the chemical fertilizers industry in Police (Figure 1). This is the main source of water suspended phosphorus in the area.

The study area was shaped during the last glaciation and postglacial period. The Holocene sediments dominate and are represented mainly by diluvial tills, sands, silty sands and peat bogs sediments. The lowest parts of terrain along the Odra River valley are covered with organic deposits (peats and peaty muds). The river flood plains and peat bogs surround the water body mainly from the east and west. Peat outcrops occur at heights up to 1 m a.s.l., in some cases even higher, forming in the small river valleys and incisions, even at an altitude up to 5 m a.s.l. Peats form mainly low bogs and, less frequently, high bogs [35] (Figure 2a).

The local river-flood plains rise up 20 m a.s.l. and were created as a result of the slow water outflow due to the melting of “dead ice” during the last glaciation. Deglaciation processes changed the water regime and induced the accumulation of sediments at the terraces of different heights. The plains are separated with numerous aeolian forms, depressions and narrow valley incisions [35].

There are several small rivers, bays, and islands located in the study area (Figure 1). The rivers are often connected with each other, and with the Odra River, by a complex of irrigation canals, discharging mostly to the Roztoka Odrzańska and Stepnicka Bay. The anthropogenic Chełminek Island was formed as a result of the dredging of the water track from Szczecin to Świnoujście and dumping the excavated sedimentary material, which started in 1889 [36].

The mean level of surface water outflow of the Odra river section nearby the Roztoka Odrzańska is very small and equals to 0.0015‰ [37]. The average volume of water discharging from the Odra to the Roztoka Odrzańska is around 500 m³/s [38]. The rip crevices have definitely also had a great impact on the changes of the water level in the Odra River system [39].

The surface and bottom water of the Roztoka Odrzańska are usually warmer by 0.5 to 1.0 °C and 0.1 to 0.4 °C, respectively, compared to the Szczecin Lagoon. The salinity is around 0.1 to 0.4‰ and is lower than in the Szczecin Lagoon. The water oxidation is worse than in the Szczecin Lagoon and drops from 8 to 5 mg/dm^{−3} O₂(dis.) at the bottom. The water is also slightly less alkaline compared to the Szczecin Lagoon, and reaches 7.15 to 8.8 pH [40].

The general chemical quality of surface water is bad or below good. The groundwater show highly elevated concentrations of Fe²⁺, Mn²⁺, and Cl[−] [41]. The total groundwater mineralization in the area of Stepnica and Police is high and ranges from 300 to 3000 mg/dm³. The dominating macro-components are Ca²⁺ (23% to 40% mval), HCO₃[−] (23% to 50% mval), and Cl[−]. The contents of Mg²⁺ and SO₄^{2−} are generally lower, 2–10% mval and 5–25% mval, respectively. The phosphorus content range is high, usually 0.7–3.0 mg/dm³, and in some areas even higher. The Zn²⁺ content is usually between 0.99 and 5.00 mg/dm³.

The pH of the groundwater is between 6 and 7. The total iron concentrations are high, usually around 0.50 to 5.50 mg/dm³. The Mn²⁺ content is usually around 0.1 mg/dm³. The dissolved silica SiO₂ is between 16.3 and 22.9 mg/dm³, and only in the northern part (around Stepnica and Gąsierzyno) these values are elevated (>29.5 mg/dm³). The Al³⁺ concentration is often <0.3 mg/dm³. The total hardness of the groundwater spans from 400 to 600 mg CaCO₃/dm³ [42].

The contamination of surface water and sediments in the Roztoka Odrzańska is well documented and associated with anthropogenic impacts. The Odra River flowing by the Roztoka Odrzańska, transports contaminants from the south, from the heavily urbanized areas. The main local areas of pollution are located nearby the harbor of Szczecin and the chemical factory in Police.

In the bottom sediments, pollution accumulates mainly due to wastewater input, mostly industrial and municipal, and less from surface runoff. The concentration of pollutants in the bottom sediments is mainly related to the river transport mechanisms, sorption potential of fine-grained and organic-rich sediments or physical and chemical properties of sediments, such as solubility, pH, and redox potential [43].

The surface sediments from the local rivers are characterized by mean variable concentration of: Ca (0.6–1.23%), Mg (0.03–0.08%), Fe (0.87–0.96%), Mn (229–1287 ppm), P (0.08–0.1%), S (0.047–0.193%),

and Zn (28–37 ppm). The mean contents of metals in the Szczecin Lagoon are 1.67% of Ca, 1.18% of Fe, 0.05% of Mg, 212 ppm of Mn, 0.027% of P, 0.041% of S, and 247 ppm of Zn. Sediments show traces of Cr in a range of 2–4 ppm [44]. The detailed geochemical data of surface sediments and water from the area of Rostoka Odrzańska/small local rivers are presented in Table 1.

The Rostoka Odrzańska sediments are mainly gyttja or sapropel muds with more than 50% of the silty-clayey fraction (Figure 2b). The iron content and heavy metals contamination (Figure 2c,d) is especially high in the uppermost 25 cm of sediments and includes elevated values of cadmium, copper, zinc, lead, cobalt, and mercury [32]. The sediments show also high contents of magnesium, potassium, and manganese [45]. Additionally, the increased concentration of heavy metals was detected in the shells of mollusks [46].

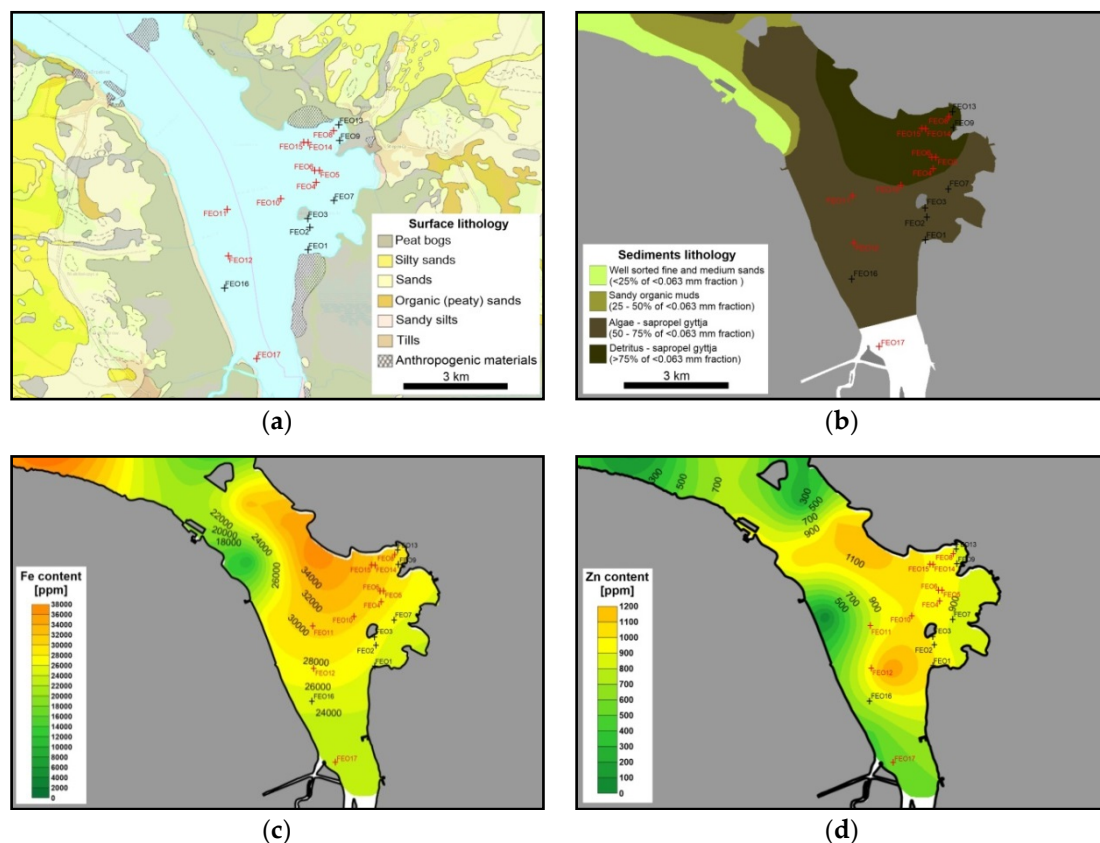


Figure 2. Location of the study area: (a) lithogenetic map of Poland; source [47]; (b) surface sediments map of the Rostoka Odrzańska; (c) map of iron content distribution in the surface sediments of the Rostoka Odrzańska; (d) map of zinc content in the surface sediments of the Rostoka Odrzańska. Red sampling sites mean sediments where pisolith nodules are found; black dots are stations without micronodules.

Table 1. Selected geochemical parameters of surface sediments and water from the area of Roztoka Odrzańska; after [44].

Surface Sediments	Al	Ca	Mg	Fe	P	S	Mn	Cr	Zn	pH/cond.
	(%)					(ppm)				(mS/cm)
Gunica	0.12	1.23	0.08	0.87	0.085	0.047	283	2	33	-
Gowienica	0.14	0.60	0.04	0.95	0.080	0.073	1287	2	28	-
Krępa	0.19	0.79	0.03	0.96	0.100	0.193	229	2	37	-
Odra	0.28	1.27	0.09	1.38	0.101	0.134	634	10	152	-
Szczecin Lagoon	0.08	0.94	0.05	0.28	0.027	0.041	212	2	60	-
Surface Water	Al	Ca	Mg	Fe	SiO ₂	SO ₄	Mn	Cr	Zn	pH/cond.
	(ppm)					(ppb)				(mS/cm)
Gunica	<0.05	116	9.7	0.26	12.5	142	369	<4	<5	7.5/1.54
Gowienica	<0.05	75	5.2	0.36	9.6	65	217	<4	<5	7.2/0.51
Krępa	0.11	51	3.2	0.44	11.0	59	172	<4	<5	4.1/0.44
Odra	<0.05	75	12.1	0.04	3.5	105	75	<4	6	7.9/0.78
Szczecin Lagoon	<0.05	92	14.8	1.00	13.1	86	247	<4	<5	8.4/2.05

3. Materials and Methods

The sediments containing pisolith nodules were collected from the eastern part of Roztoka Odrzańska, Odra river, northern Poland. The samples were taken directly from the water, using a Van Veen sludge trap deployed from a catamaran “Szuwarek.” To determine whether the sediments contain some micronodules, samples were flushed using a 4 mm sieve. The shells and plant debris was removed using a 500 µm sieve. The material remained in the 500 µm sieve was described and pisolith nodules were separated. Photographs were taken using a Zeiss Stereo Discovery.V20 stereoscopic microscope with PlanApo S1.0 lens, smooth adjustment, Canon EOS 500D camera and AxioVision (Rel. 4.8. Edition) software. Sediment sampling, preparatics, and photographs were taken at the Institute of Marine and Environmental Sciences, University of Szczecin, Poland.

Representative pisolith nodules were analyzed using the SEM-energy dispersive x-ray (EDX) method at the Polish Geological Institute—National Research Institute, Holy Cross Mts. Branch in Kielce, Poland. Hitachi TM 3030 scanning electron microscope, equipped with the Thermo EDS detector Noran System 7 was used. An acceleration voltage of 15.0 kV was applied. Additionally, samples were covered by carbon coating using the Cressington 108 carbon sprayer. For this reason, and also due to samples immerse in epoxide resin, the total C content was omitted in the analysis. In the case of >10% of carbon, the results were included in the chemical data. The results obtained allowed a chemical recognition of minerals. The structural water content H₂O[−] was calculated from stoichiometry. The chemical data were the basis for the calculation of metal ratios, such as Fe/Mn, P/Fe, Ca/Mg, Si/Al, or Fe/S.

Additionally, few crushed pisoliths were analyzed using XRD (Faculty of Chemical Technology and Engineering, West Pomeranian University of Technology, Szczecin). The pulverized nodules were investigated using a PANalytical Empyrean II diffractometer. The CuKα₁ (1.540598Å) radiation, the voltage of 35 kV, and beam intensity of 30 mA, measuring angles range 5–70° 2θ and step of 0.02°/2 s were applied. The device was equipped with a graphite monochromator and PIXcel 3D strip detector. In addition, the Ni-β filter and spinner (1 sample rotation per 16s) were implemented.

The qualitative and quantitative identification of minerals was made using the Match! 3 software and the COD-Inorg REV214414 database (state of records on 29 March 2019) [48]. The number of mineral phases was estimated with the Rietveld refinement and FullProf software.

As the reference material for the Odra River hydrological system and analyzed pisolith nodules, we investigated and described previously unknown nodules from the Dąbie Lake and middle part of the Szczecin Lagoon. These samples were collected also directly from the water in 2009–2011. Additionally, we compared results obtained with archival data of the lake, lacustrine and riverine

nodules, bog ores, selected P- and Fe-rich minerals, siderite ores, organic sediments, polymetallic nodules, and Baltic Sea nodules (Appendix A).

4. Results

The loose pisolith micronodules were found in the surface sediments of the Roztoka Odrzańska within 10 of 17 sampling stations (Figure 2a). The material was found in the gyttja and sandy gyttja/sandy sapropel muds, including also the shells of *Dreissena polymorpha*, fragments of plants, quartz grains, scales, skeletal remnants of fish, spores, and peat fragments.

4.1. General Description

The two major textural types of pisolith nodules were identified: (i) soft and porous, spherical, 0.2 to 0.5 mm in diameter, covered only by a thin rust-yellowish cortex, composed of weathered hematite or limonite, disintegrating even after a slight touch, with no distinctive geometric internal texture, nuclei, and layering (Figure 3a–d); (ii) solid, with well-developed cortex, concentric layering and nuclei, in few cases with the septarian-type cracks inside the nucleus (Figure 4a–f). The type (i) was identified in nine samples and type (ii) only in one (FEO8).

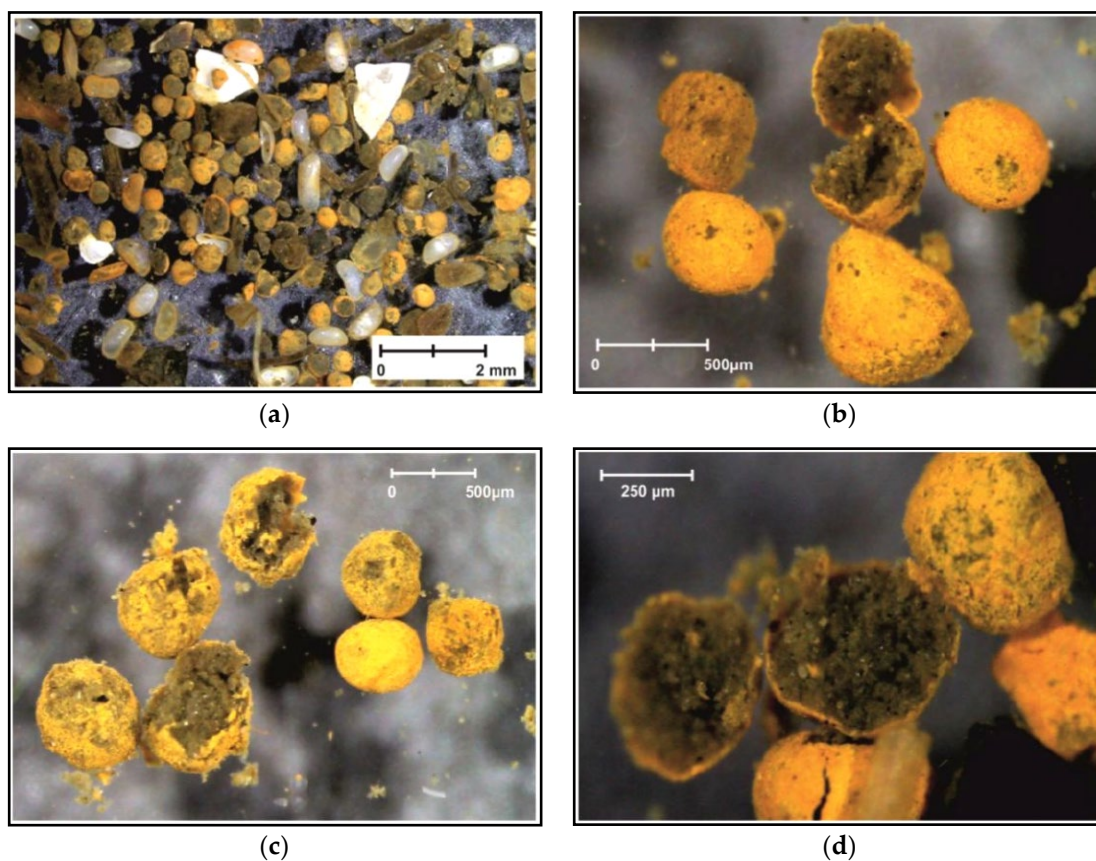


Figure 3. Examples of loose, soft and earthy spherical micronodules collected from the FEO4 sampling site (a–d). The interior shows a highly porous texture, composed mainly of goethite, with traces of phosphates, and carbonates. The thin yellowish cortex developed as an oxidation layer composed of limonite or hematite.

The greatest amount of best-preserved pisolith micronodules were found in the FEO8 sample, where we counted 165 whole nodules, 19 broken, and 7 halves. Specimens varied of size from 0.5 to 2 mm and showed spherical or oval forms. Some nodules were broken and cracked, mostly due to the drying and loose of water due to the dehydration of external layers (Figure 4). In some cases,

blueish oxidized surfaces of phosphate minerals were identified (Figure 4e). Almost all of the broken micronodules showed the presence of a nucleus, mainly of detrital origin, such as quartz or feldspar (Figure 4f).

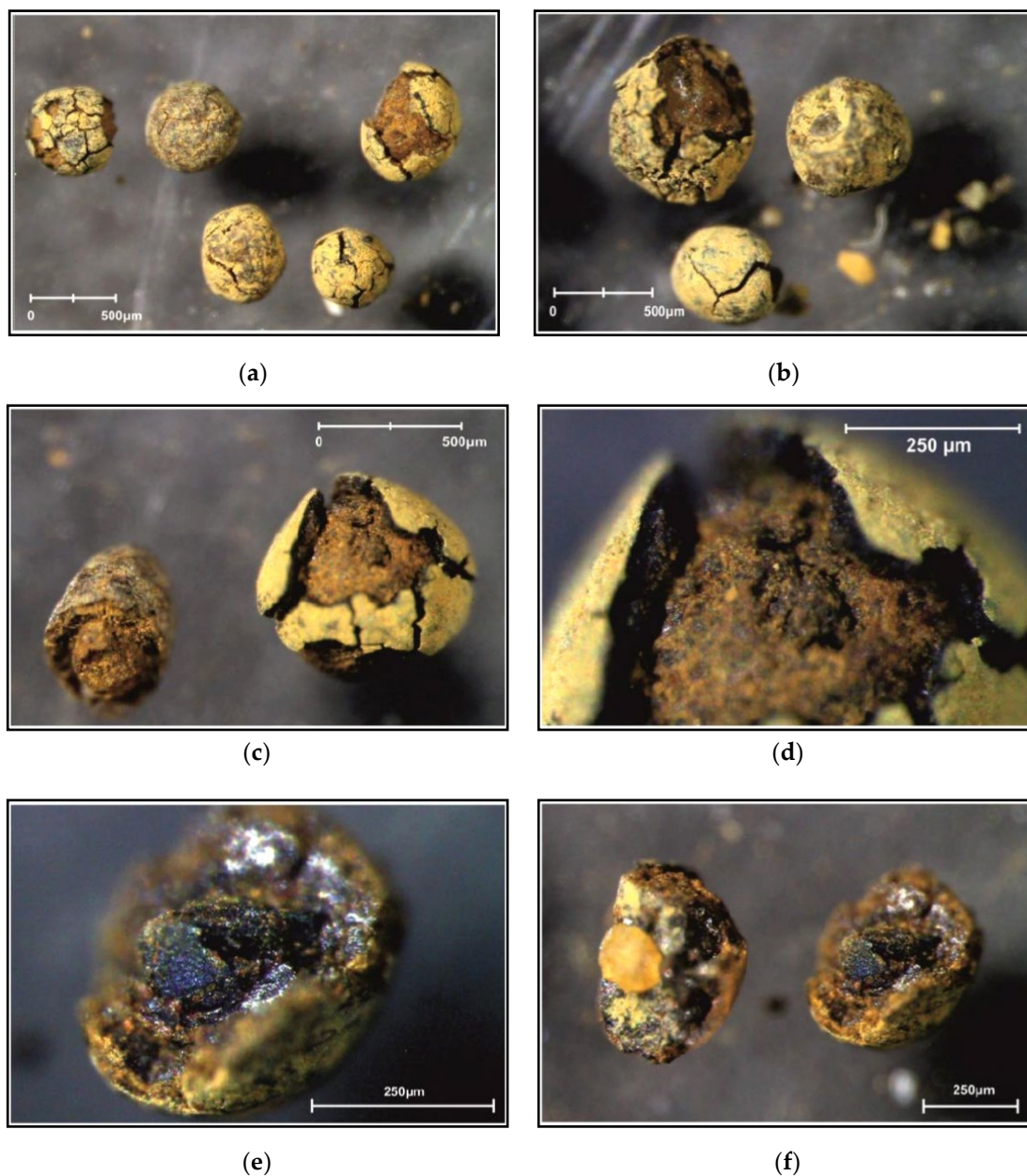


Figure 4. Examples of loose, solid spherical micronodules collected from the FEO8 sampling site. The thin and radially crushed yellowish cortex developed as an oxidation layer built of limonite and hematite. Interior shows the presence of solid authigenic nucleus (massive iron oxyhydroxides or siderite; (a–e) or detrital one (f). In some cases, septarian-type cracks were observed.

4.2. XRD

According to the XRD bulk powder analysis of selected micronodules (Figure 5), several minerals were identified (Table 2). Among them, the Fe-hydroxides and Fe-oxides, typical of aerobic environments, dominate:

1. goethite showing several but non-distinctive chemical substitution [49];
2. proto-hematite [50];

3. hematite with isomorphous substitutions (contaminated) [51];
4. lepidocrocite [52];
5. ferrihydrite [53];
6. traces of native Fe [54].

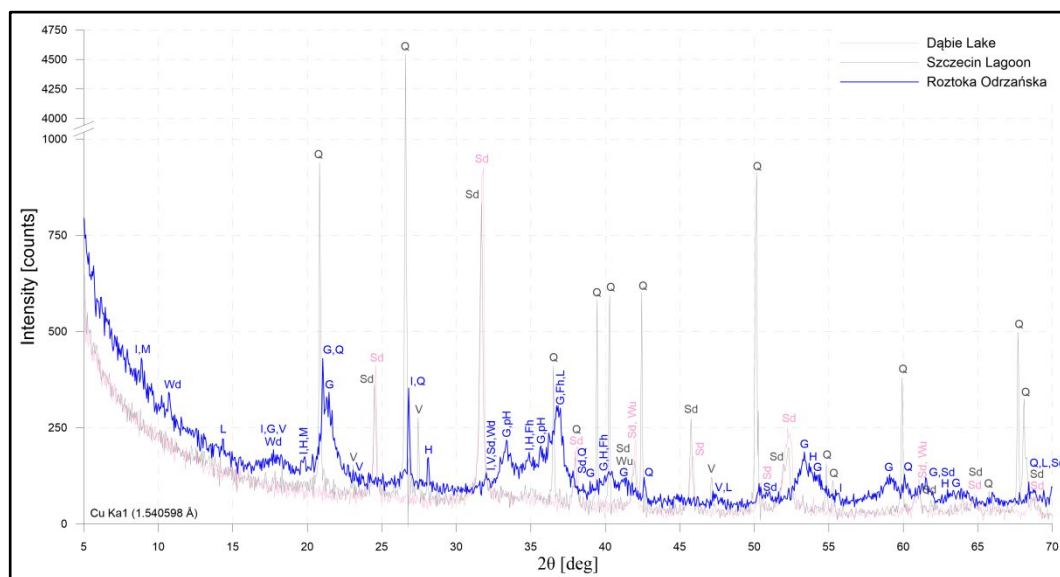


Figure 5. Representative XRD powder diffractograms of the FEO8 sample from the Roztoka Odrzańska, and reference nodules from the Dąbie Lake and Szczecin Lagoon. The identified minerals are Q—quartz, G—goethite, H—hematite, pH—proto-hematite, L—lepidocrocite, Fh—ferrihydrite, V—vivianite (metavivianite), Sd—siderite, I—illite, M—montmorillonite (Fe—smectite), Wd—woodwardite (Zn—woodwardite), and Wu—wüstite.

In the group of phosphates, the hydrated Fe-phosphate in a type of metavivianite (Fe^{3+}) and vivianite (Fe^{2+}), typical for oxygen-rich environments [55,56] was identified. Additionally, the β -quartz was identified and traces of Fe-carbonates, mainly in siderite type [57]. Clay minerals include illite and Fe-smectite, with the domination of illite [58,59].

The chemically most complex are mixed and hydrated sulfates, carbonates, or sulfo(carbonates), best matching for woodwardite and zincwoodwardite [60,61]. These minerals are products of decomposition of, most likely, anthropogenic products, such as industrial dust or trails. Their presence was confirmed by the SEM-EDX analysis.

The XRD analysis indicated the presence of feldspar, zircon and other less frequent debris minerals found during SEM-EDX was not confirmed. The traces of decomposing chromium minerals, most likely weathering spinels or some anthropogenic products, were not visible.

The XRD data of Roztoka Odrzańska pisolith nodules, compared to micronodules from the Dąbie Lake and Szczecin Lagoon, indicate significant differences (Table 2). The Szczecin Lagoon sample is dominated by quartz (78.9%) and siderite (18.5%), with traces of vivianite or metavivianite (1.8%), and wüstite (<1%). The nodules from the Dąbie Lake are dominated by Mn-substituted siderite (88.4%) [62], with admixture of quartz (10.0%), traces of wüstite (1.5%) [63], and native iron (<1%).

Table 2. The XRD data of the FEO8 bulk micronodules from the Roztoka Odrzańska, Odra River, NW Poland. Additionally, the reference nodules from the Dąbie Lake and Szczecin Lagoon are included.

Identified Minerals with Theoretical Chemical Formula	Content (%)		
	Roztoka O. (FEO8)	Dąbie Lake	Szczecin Lagoon
quartz β -SiO ₂	7.0	10.0	78.9
goethite α -FeO(OH)	29.8	-	-
hematite Fe ₂ O ₃	6.5	-	-
wüstite FeO	-	1.5	traces ¹
proto-hematite Fe _{1.9} H _{0.06} O ₃	6.4	-	-
lepidocrocite γ -FeO(OH)	2.7	-	-
ferrihydrite (Fe ³⁺) ₂ O ₃ ·0.5H ₂ O	5.5	-	-
native iron Fe	traces ¹	traces ¹	-
vivianite-metavivianite Fe ²⁺ Fe ²⁺ ₂ (PO ₄) ₂ ·8H ₂ O	9.7	-	1.8
Fe ³⁺ ₂ (PO ₄) ₂ (OH) ₂ ·6H ₂ O			
siderite FeCO ₃	4.3	88.4 ²	18.5
illite K _{0.6-0.85} Al ₂ (Si,Al) ₄ O ₁₀ (OH) ₂	26.1	-	-
montmorillonite (Fe-smectite)			
(CaO _{0.5} ,Na) _{0.3} Fe ³⁺ ₂ (Si,Al) ₄ O ₁₀ (OH) ₂ ·nH ₂ O	1.4	-	-
woodwardite-zincwoodwardite Cu ₄ Al ₂ (SO ₄)(OH) ₁₂ ·2–4(H ₂ O)	traces ¹	-	-
[Zn _{1-x} Al _x (OH) ₂][(SO ₄) _{x/2} (H ₂ O) _n]			

¹ Minerals with content <1%; ² Around 10% of siderite show increased contents of Mn (potential admixtures of rhodochrosite).

4.3. SEM-EDX Analysis

The SEM-EDX analysis reveals concentric textures and a frequent presence of solid nuclei, admixtures of detrital material, such as quartz, K-feldspar or zircon, remnants of chromium minerals, and others (Figure 6a–e). Cortex is composed mainly of Fe-hydroxides in a type of goethite, with smaller content of hematite. Hematite was discovered mainly as an oxidation layer developed in a form of coating covering nuclei, or a very thin external layer.

According to the results of the SEM-EDX chemical analysis (Table 3), the individual pisoliths are dominated by Fe-oxyhydroxides in a type of goethite (or lepidocrocite). The identified Fe-hydroxides show a low structural deficiency in Fe³⁺ (~9%), being substituted mainly by Si, P, Al, and Ca. Additionally, vacancies of Mn, Mg, S, V, Zn, and F were observed. The mean calculated H₂O⁻ content is 13.83%. The hematite was identified as a minor component and shows greater vacancies of Si, P, Ca, Al, and S. Similarly to goethite, hematite indicates phosphatization and traces of S. The nuclei of analyzed pisoliths are composed of some debris minerals, like quartz, K-feldspar, zircon, Cr-spinel and non-defined Fe-Cr-Si phase. Besides this, some mixed Zn-sulfo(carbonates), which show some chemical similarities to woodwardite or Zn-woodwardite, are found. Woodwardite and its Zn-rich analog are often associated as a by-product of industrial materials.

All identified Fe-hydroxides show higher than theoretical content of structural water, which may be evidence of chemical decomposition processes occurring in the water environment. Additionally, the higher vacancy and substitution by alkali or Si+Al indicates pisolith formation in the sedimentary environment.

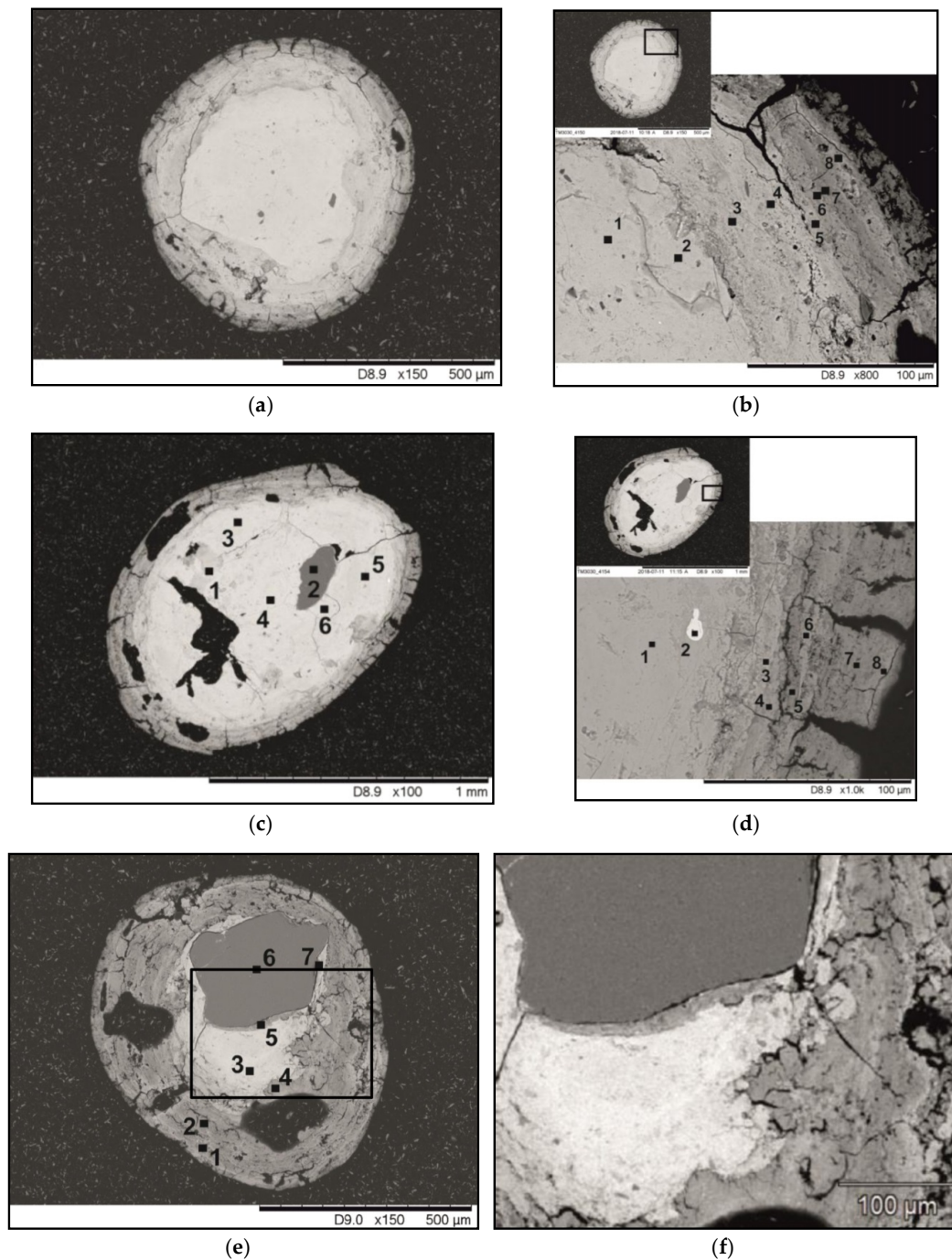


Figure 6. Representative SEM photos and energy dispersive x-ray (EDX) data points of pisolith nodules from the Rostoka Odrzańska: (a) round micronodule with solid detrital quartz nuclei (1), surrounded by goethite coating (b; 2–8); slight Si and Ca content increase towards crushed edges and highest Fe contents in points 6–7; (c) oval pisolith nodule with quartz debris (2) and goethite core (1, 3–6); empty spaces after loose grains and subtle internal crushes; more distinctive laminae-like external layer; (d) laminated and radially crushed external layer composed of goethite (1, 4, 6, 8), hematite (3 and 7) and detrital zircon (2); intermixtures of non-identified Zn-rich sulpho(carbonates) (5); (e) micronodule with distinctive two layers composed of goethite (1–5), detrital quartz (6) and non-identified Cr-rich minerals, probably remnants of Cr-rich spinels or Cr-phylosilicates (7); zone of increase in Fe content and decrease with H_2O^- and Al (1 to 5); (f) zoom on transition of quartz nucleus and goethite.

Table 3. Mean SEM-EDX chemical data of selected pisolith micronodules from the Roztoka Odrzańska, Odra River, NW Poland.

	Fe-hydroxides Fe ³⁺ -H ₂ O ⁻ N = 43	Hematite Fe ³⁺ -O ₂ ⁻ N = 3	K-Feldspar N = 2	Zircon N = 1	Wdw/Zn-Wdw ² Zn ²⁺ -CO-H ₂ O ⁻ N = 2	NI ³ Fe-Cr N = 3	NI ³ Si-Cr-Fe N = 2
SiO ₂	4.95	7.93	57.69	23.15	4.97	10.06	53.18
Al ₂ O ₃	0.76	0.69	18.27	-	0.73	0.19	-
MgO	0.18	-	-	-	-	-	-
CaO	2.35	2.91	-	-	1.73	1.54	-
Na ₂ O	traces ¹	-	-	-	-	-	-
K ₂ O	-	-	20.04	-	-	-	-
MnO	0.35	-	-	-	-	0.52	-
FeO _t	-	-	4.01	5.03	24.58	72.17	3.61
Fe ₂ O ₃	80.89	84.90	-	-	-	-	-
Cr ₂ O ₃	-	traces ¹	-	-	-	4.68	15.60
V ₂ O ₅	traces ¹	-	-	-	-	-	-
ZnO	traces ¹	-	-	-	11.94	-	-
P ₂ O ₅	4.79	3.22	-	-	2.30	3.33	0.48
ZrO ₂	-	-	-	71.81	-	-	-
SO ₂ ⁻	0.23	0.35	-	-	9.27	-	-
CO ₂ ⁻	-	-	-	-	22.67	-	23.13
F ⁻	traces ¹	-	-	-	-	-	-
H ₂ O ⁻	13.83	-	-	-	21.81	7.50	-

¹ Traces (usually ~0.1%) found only in single EDX analyses; ² woodwardite and Zn-woodwardite;

³ non-identified (NI).

The individual layers of Fe-hydroxides and Fe-oxides indicate intermediate iron content (50 to 65%), with a mean of 56.6% (Figure 7). The manganese substitution is low and below 0.2%, with a mean of 0.3%. Only a few goethite data points show Mn incorporation elevated to 0.8 to 1.0%. All samples show increased phosphorus contents (1.8 to 2.2%), with a mean of 2.0%. Additionally, the chemical analysis indicates the dominance of Si over Al. The mean silica content is 2.7%, with few internal layers of goethite and hematite showing values elevated >3.5%. The Al content is low and rather evenly distributed in all samples; the mean is 0.4% and maximum values up to 0.8%. The SEM-EDX data points show Ca dominance over Mg. The mean Ca content is 1.8%, with a maximum of 4.2%. The distribution shows two modes, 1.0% and 2.2%, respectively. Only two data points indicated Ca values above 3.6%. The mean Mg content is low and equals to 0.18%. The mean structural water H₂O⁻ amount calculated from the stoichiometry is 13.9%. Samples show trace contents of Na and K, 0.17% and <0.10%, respectively. The total alkalinity, calculated as a (CaO + MgO)/SiO₂, is 0.17.

The mean Fe/Mn ratio equals 385 and P/Fe is 0.04. The mean Ca/P ratio is 0.89 and Ca/Mg equals 11.42. The Si/Al ratio is 43.36. The Fe/S ratio calculated basing on 12 measurements is 167.17.

The pisolith nodules from the Roztoka Odrzańska indicate similar geochemical signatures to bog ores. According to the SiO₂/P₂O₅ ratio, the EDX data samples are closer to pure Fe-oxides and Fe-hydroxides, compared to typical hematite rich ochres, siderite nodules or highly phosphatized Fe-rich precipitates (Figure 8). Compared to phosphate-rich nodules and bog ores, samples from the Roztoka Odrzańska indicate low phosphorus contents and only slight siderization. These results are in good correspondence with XRD data.

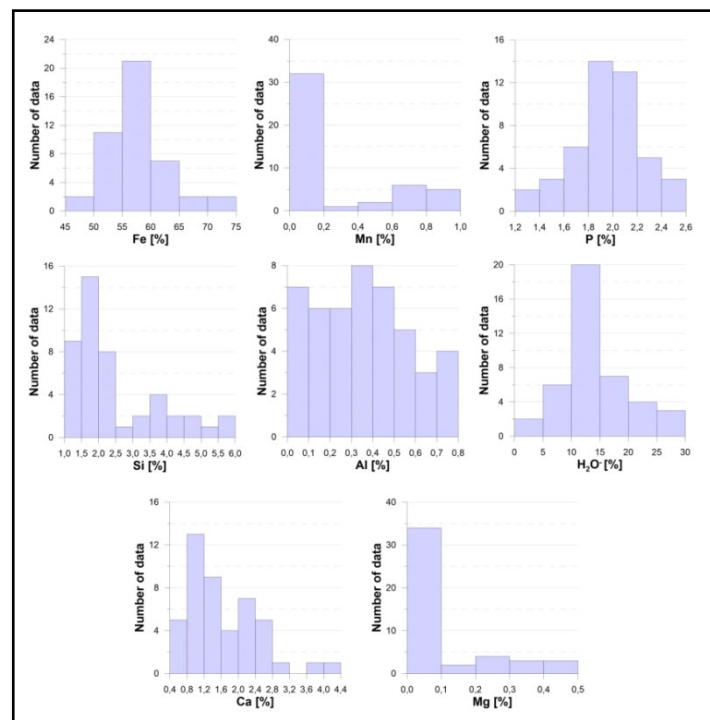


Figure 7. The SEM-EDX chemical variability of ferruginous micronodules from the Rostoka Odrzańska, Odra river, NW Poland. Structural water H_2O^- content calculated from the stoichiometry.

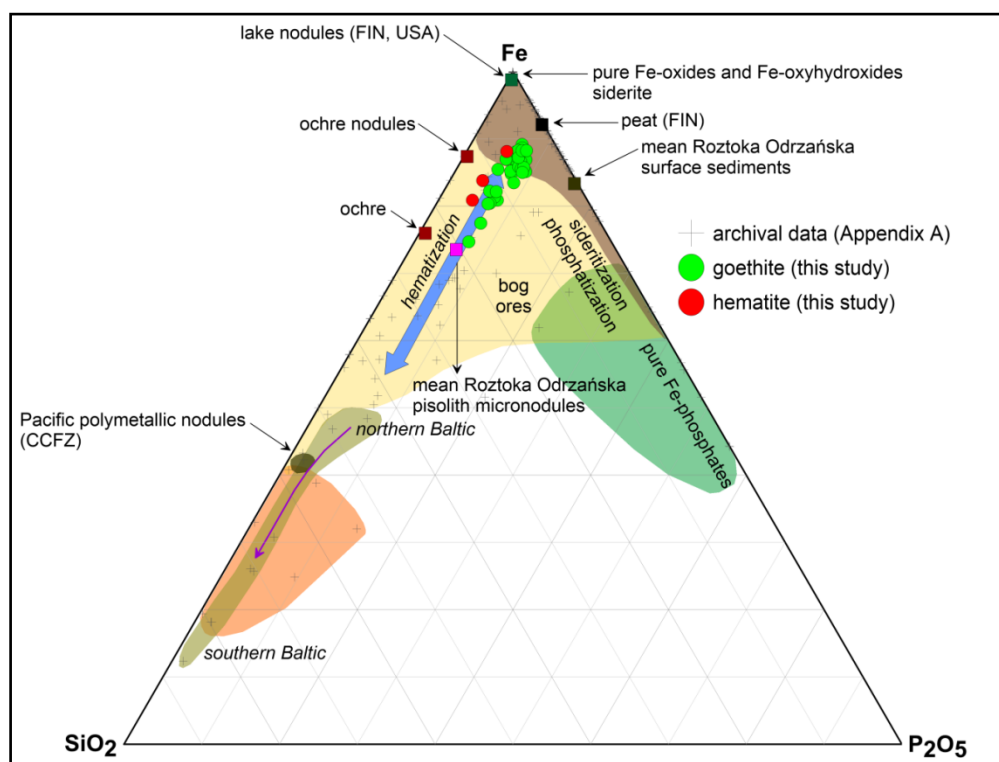


Figure 8. Discriminative ternary diagram compiled with data of the Rostoka Odrzańska nodules and archival geochemical results of different kinds of Fe-rich precipitates, selected rocks, sediments, and minerals. For the detailed description see Appendix A.

5. Discussion and Conclusions

The morphological, chemical, and mineralogical variability of pisolith nodules from the Róztoka Odrzańska is closely related to the environmental conditions, characterized by high trophic level, presence of nutrient-rich peat bogs, good oxygenation and presence of glacial debris material (sands and silts). The Fe-dominated pisolith nodules were found in the small and shallow bay, among organic-rich sapropel muds, where the increased inflow of river water occurs and intensive drainage of the adjacent area is observed (Figure 9). The pH level of the Odra River, Szczecin Lagoon, and other small rivers are usually higher (7.2–8.4) compared to peats and organic sediments located within the area (usually <6), which provides good conditions to precipitation of iron compounds.

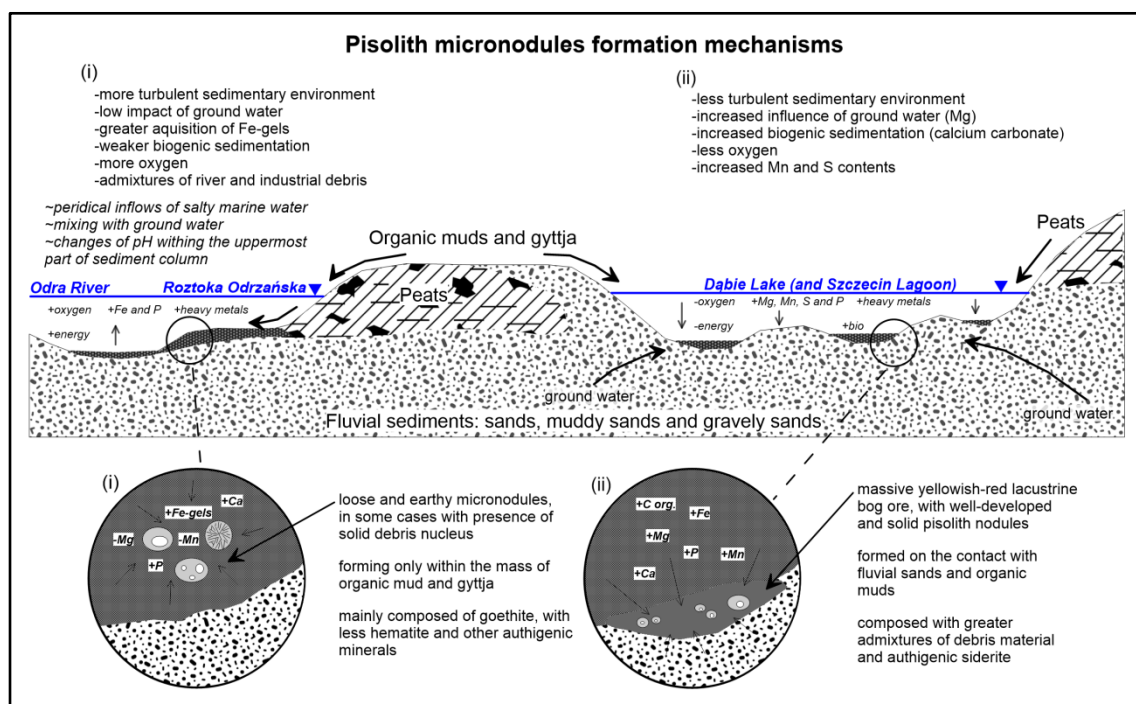


Figure 9. Discriminative ternary diagram compiled with data of the Róztoka Odrzańska nodules and archival geochemical results of different kinds of Fe-rich precipitates, selected rocks, sediments, and minerals. For the detailed description see Appendix A.

Described nodules were formed as a result of the precipitation of Fe-rich hydroxides, dominated by goethite, directly into the sediments. The iron source may be connected with nearby located peat bogs, soil processes or Fe-gels transported by the Gowienica river. Goethite usually forms in moist and highly oxidizing conditions. The presence of ferrihydrite, proto-hematite, and hematite is connected with further oxidation that might have taken place especially after the removal of the samples from the water, and the formation of the thin external cortex. These changes are also highlighted by cracking of the external layer, mainly due to some loss of structural water. Small admixtures of siderite suggest formation in freshwater, poor with sulphur, however rich in other organics [64]. Siderite forms when goethite (or lepidocrocite) is reduced by the decomposition of organic matter. Phosphorus incorporated within vivianite or metavivianite supposedly comes as a nutrient-rich drainage product, rather than weathering material [65,66].

The elevated contents of Al, Ca, Mg, Fe, and Mn in peat and sediments of the Róztoka Odrzańska are typical indicators of the organic-rich sedimentary environment. Additionally, the high P and S concentrations are natural and typically associated with organic sediments, however, some input from the Police fertilizer industry is also significant, being transported directly by the Odra river few

kilometers north to the Roztoka Odrzańska, mixing with small drainage rivers cutting peats and gyttja sediments. The area of Roztoka Odrzańska is composed mainly of slightly acid soils ($\text{pH} > 6$).

The composition of surface and groundwater indicate a typical inflow of freshwater sources. The marine input is visible rather in the northern part of the Szczecin Lagoon, however occasional marine water inflows were noted even in the deeper part of the Odra River system. Mixing of salty and groundwater affect cyclic, short-scale environmental changes of selected physicochemical parameters, especially pH and oxygenation, which potentially may induce Fe-precipitation, nucleation, and growth of pisolith nodules.

Some spots of more acidic soils and water may be connected with spots of anthropogenic materials. The greater ratios of Fe/S and P/Fe in the Roztoka Odrzańska pisolith nodules, compared to micronodules from the Dąbie Lake and Szczecin Lagoon, suggest greater phosphorus release potential and lower impact on the formation of nodules [67]. The fractionation of P/Fe ratios in surface sediments are strongly related to winter-summer cyclicity and changes of oxygen conditions [68]. The Police chemical industry phosphorus impact on the formation of nodule shall be part of further environmental studies.

The greater amount of detrital material inside micronodules (quartz, feldspar, zircon) and clays additionally confirm the precipitation of Fe-rich hydroxides in an oxygenated environment of increased water discharge. The increased content of phosphorus and presence of fresh blueish vivianite (or metavivianite) found inside pisoliths suggest diagenetic transformations due to the oxygen depletion. Increased contents of Si, compared to Al, and expressed by Si/Al ratio ~ 44 , suggests automorphic formation. The elevated amount of silica may not be connected only with the detrital quartz, but also with the colloidal organic matter (i.e., diatoms) dispersed in draining water [44].

Elevated concentrations of Zn and other heavy metals are associated mainly with the pollution transported by the Odra River from Police and southern Poland. However, the high contents of heavy metals are also associated with organic sediments of the Roztoka Odrzańska and peats of the neighboring areas, which are normally accumulated by natural processes [69]. One of the most problematic questions is, whether the presence of Zn-rich sulfo(carbonates) is a result of chemical weathering of anthropogenic slags or industrial dust included as internal debris in analyzed nodules, or whether these are natural decomposing minerals.

Compared to the Roztoka Odrzańska, the reference nodules from the Dąbie Lake are dominated by primary siderite and Mn-substituted siderite, potentially even with a small amount of rhodochrosite. The presence of Mn-carbonate or greater Mn-(Mg) substitution in the chemistry of siderite and calcite is related to diagenesis in brackish conditions and the authigenic formation of components of fresh-lake sediments [70]. Admixtures of FeO (wüstite) may indicate the low influence of reductive processes. The low amount suggests formation in a more stable, well-oxygenated, and freshwater environment, compared to the Roztoka Odrzańska [71]. The greater amount of siderite in the Dąbie Lake micronodules may be connected with worse trophic conditions, where CO_2 is produced more intensively, due to increased decomposition of organic matter.

The loose and earthy spherical micronodules from the Roztoka Odrzańska were supposedly formed due to subaqueous authigenesis, dominated by Fe-oxyhydroxides, low amount of hematite, clay minerals, and presence of highly porous textures (compare i.e., [72]).

Morphological features of analyzed nodules suggest a rather fast growth (nucleation) rate, which shall be confirmed by additional isotopic studies and age estimation.

Studies of textures, mineralogy, and geochemistry of less known lacustrine pisolith nodules provide valuable information on sedimentary environmental conditions and regolith studies. Changes of metal and biogenic elements concentrations affect the early diagenetic formation of different types of micronodules. Highly organic Quaternary limnic or fluvial sediments are especially susceptible to authigenic growth, additionally supplied by admixtures of debris material. In some cases, the core of solid lacustrine micronodules may be composed even of material indicating anthropogenic signatures, often showing traces of intensive chemical decomposition.

Author Contributions: Conceptualization, U.R., Ł.M., and A.S.; methodology, U.R., Ł.M., A.S., and S.S.; software, U.R., Ł.M., and S.S.; validation, Ł.M. and A.S.; formal analysis, A.S. and Ł.M.; investigation, U.R. and S.S.; resources, A.S., S.S., and Ł.M.; data curation, U.R., Ł.M., and S.S.; writing—original draft preparation, Ł.M. and U.R.; writing—review and editing, Ł.M., U.R., and A.S.; visualization, Ł.M. and U.R.; supervision, A.S.; funding acquisition, Ł.M., A.S., and S.S. All authors have read and agreed to the published version of the manuscript.

Funding: This research was financed by the Institute of Marine and Environmental Sciences, University of Szczecin, Poland statutory funds and sources of Polish Geological Institute—National Research Institute, Holy Cross Mts. Branch in Kielce, Poland.

Acknowledgments: We would like to thank Kamila Mianowicz, PhD (University of Szczecin), for linguistic assistance. We are grateful to prof. Ryszard K. Borówka and Dominik Zawadzki, PhD (University of Szczecin), for providing reference nodule samples from the Dąbie Lake and Szczecin Lagoon. Additionally, we would like to thank prof. Rafał J. Wróbel (West Pomeranian University of Technology) for XRD and XRF analysis. Finally, we would like to thank two reviewers for their positive feedback and valuable comments.

Conflicts of Interest: The authors declare no conflict of interest. The funders had no role in the design of the study; in the collection, analyses, or interpretation of data; in the writing of the manuscript, or in the decision to publish the results.

Appendix A

Table A1. Archival data of the lake, lacustrine and riverine nodules, bog ores and other Fe-rich precipitates (see Figure 5).

Location and Type	SiO ₂	P ₂ O ₅	Fe	Mn	Ca	Mg	S	Fe/Mn	Ca/Mg	P/Fe	Fe/S	(CaO+MgO)/SiO ₂	Data Source (See References)
			(%)					-	-	-	-	-	
Satterhutte, Krzyż, POL (bog ore)	3.90	0.98	41.90	1.90				22.05		0.010			[3]
Wisła, Wisłok and San river valleys, POL (bog ore)	19.35	2.14	28.69	2.89				9.93		0.033			[3]
Biłgoraj-Tomaszów Mazowiecki, POL (bog ore)	21.00	1.12	29.32	3.00				9.77		0.017			[3]
Kalisz-Konin-Turek, POL (bog ore)		5.89	42.39	1.62				26.17		0.061			[3]
Mława-Lomża, POL (bog ore)	11.83	3.64	34.38	0.75				45.84		0.046			[3]
Upper Silesia, POL (bog ore)	28.10	0.25	36.04	1.20				30.03		0.003			[3]
Wieluń, POL (bog ore)	18.55	2.80	41.69	0.86				48.48		0.029			[3]
Mazowieckie Voivodeship, POL (bog ore)		0.04	29.53	2.43				12.15		0.001			[3]
Łódzkie Voivodeship, POL (bog ore)		8.06	31.14	2.79				11.16		0.113			[3]
Glinne, POL (bog ore)	30.11		30.11	2.11	1.03		0.14	14.27			209.1	0.048	[3]
Bobrowniki I, POL (rusty-yellowish bog ore)	6.84		35.55	0.27	2.02	0.13	0.19	131.67	15.91		185.2	0.444	[3]
Bobrowniki II, POL (red bog ore)	3.16		46.62	0.26	1.13	0.12	0.17	179.31	9.83		277.5	0.561	[3]
Rubinkowo I, POL (bog ore)	6.60		45.79	2.01	1.59	0.41	0.07	22.78	3.88		636.0	0.440	[3]
Rubinkowo II, POL (bog ore)	9.40		40.64	2.64	2.23	0.37	0.06	15.39	5.96		635.0	0.398	[3]
Białystok, POL (bog ore)	14.90		29.83										[3]
Lublin, POL (bog ore)	19.39		26.68										[3]
Olsztyn, POL (bog ore)	12.66		28.09										[3]
Poznań, POL (bog ore)	23.38		40.23										[3]
Rzeszów, POL (bog ore)	21.14		29.12										[3]
Mazowieckie Voivodeship, POL (bog ore)	34.49	0.84	26.97	2.01	0.50	0.05	0.08	13.42	10.00	0.014	336.3	0.023	[3]
Biedaszki, POL (bog ore)	3.03	5.19	49.60	2.67	1.69	0.15		18.58	11.27	0.046		0.863	[3]
Dąbrówka, POL (bog ore)	14.57	3.65	39.36	0.15	0.52	0.13		262.40	4.09	0.040		0.064	[3]
Dębe Małe (bog ore)	15.00	5.59	27.37	0.41	2.08	0.12		66.76	17.19	0.089		0.208	[3]
Grądy Dolne (bog ore)	22.81	2.87	30.56	9.64	1.23	0.16		3.17	7.55	0.041		0.087	[3]
Kuźnica Słupska, POL (bog ore)	7.04	10.03	27.74	0.78	2.60	0.33		35.56	7.98	0.158		0.594	[3]
Strzyżew, POL (bog ore)	1.53	2.03	36.40	0.25	0.97	0.06		145.60	16.09	0.024		0.953	[3]
Mean soft bog ores, POL	11.08	4.54	32.71	0.31	1.31	0.21		105.52	6.21	0.061		0.197	[3]
Mean solid bog ores, POL	36.89	3.52	25.63	2.48	1.05	0.18		10.33	6.00	0.060		0.048	[3]
Roztoka Odrzańska, POL (pisolith nodules)	14.04	4.11	50.42	0.28	1.52	0.16	0.72	385.45	9.50	0.036	167.2	0.170	This study

Table A1. Cont.

Location and Type	SiO ₂	P ₂ O ₅	Fe	Mn	Ca	Mg	S	Fe/Mn	Ca/Mg	P/Fe	Fe/S	(CaO+MgO)/ SiO ₂	Data Source (See References)
			(%)					-	-	-	-	-	
Ruukki-Vihanti, FIN (Fe-rich mire precipitates: black amorphous and vivianite)	4.20	2.00	43.82	0.02	0.21	0.02	0.02	2921.33	11.86	0.020	2191.0	0.079	[64]
Ruukki-Vihanti, FIN (Fe-rich mire precipitates: vivianite and sand)	35.80	9.20	21.21	0.05	0.50	0.78	0.01	461.09	0.64	0.189	2121.0	0.056	[64]
Ruukki-Vihanti, FIN (Fe-rich mire precipitates: yellow, black streaked, siderite and vivianite)	1.00	2.10	58.97	0.09	0.29	0.01	0.01	634.09	47.43	0.016	5897.0	0.410	[64]
Ruukki-Vihanti, FIN (Fe-rich mire precipitates: pale yellow, fine grained, siderite)	2.30	0.50	61.23	0.23	0.36	0.01	0.01	263.92	29.64	0.004	6123.0	0.226	[64]
Ruukki-Vihanti, FIN (Fe-rich mire precipitates: green, coarse grained, siderite)	4.60	0.30	60.06	0.14	0.21	0.02	0.01	432.09	11.86	0.002	6006.0	0.072	[64]
Ruukki-Vihanti, FIN (Fe-rich mire precipitates: pale yellow, bedded, siderite)	0.40	0.10	61.85	0.26	0.43	0.02	0.01	235.17	17.79	0.001	6185.0	1.602	[64]
Ruukki-Vihanti, FIN (Fe-rich mire precipitates: brown oxidized surface, goethite and limonite)	0.50	0.10	66.36	0.08	0.14	0.01	0.01	857.36	23.71	0.001	6636.0	0.420	[64]
Ruukki-Vihanti, FIN (Fe-rich mire precipitates: brown oxidized, fine grained with dark nodules, goethite and limonite)	2.40	1.30	62.39	0.01	0.07	0.01	0.01	8060.72	5.93	0.009	6239.0	0.050	[64]
Ruukki-Vihanti (42), FIN (Fe-rich mire precipitates: black amorphous, siderite and vivianite)		10.65	25.20	0.09	0.12	0.25	0.59	280.00	0.48	0.184	42.7		[64]
Ruukki-Vihanti (43), FIN (Fe-rich mire precipitates: black amorphous)		4.63	16.90	0.07	0.27	0.31	1.37	241.43	0.87	0.119	12.3		[64]
Ruukki-Vihanti (48), FIN (Fe-rich mire precipitates: black amorphous, siderite and vivianite)		6.05	31.50	0.10	0.24	0.36	0.10	315.00	0.67	0.084	315.0		[64]
Ruukki-Vihanti (50), FIN (Fe-rich mire precipitates: black amorphous, siderite and vivianite)		14.24	26.50	0.14	0.31	0.69	0.57	189.29	0.45	0.234	46.5		[64]
Ruukki-Vihanti (54), FIN (Fe-rich mire precipitates: black amorphous, siderite)		1.97	20.70	0.04	0.24	0.48	0.14	517.50	0.50	0.041	147.9		[64]
Ruukki-Vihanti (55), FIN (Fe-rich mire precipitates: black amorphous)		4.88	17.00	0.07	0.36	0.65	0.33	242.86	0.55	0.125	51.5		[64]

Table A1. Cont.

Location and Type	SiO ₂	P ₂ O ₅	Fe	Mn	Ca	Mg	S	Fe/Mn	Ca/Mg	P/Fe	Fe/S	(CaO+MgO)/ SiO ₂	Data Source (See References)
			(%)					-	-	-	-	-	
Ruukki-Vihanti (58), FIN (Fe-rich mire precipitates: black amorphous, siderite)		3.94	15.20	0.05	0.38	0.68	0.25	304.00	0.56	0.113	60.8		[64]
Ruukki-Vihanti (60), FIN (Fe-rich mire precipitates: black amorphous, siderite and vivianite)		16.12	26.70	0.16	0.16	0.34	0.26	166.88	0.47	0.263	102.7		[64]
Ruukki-Vihanti (63), FIN (Fe-rich mire precipitates: black amorphous, siderite and vivianite)		6.73	12.10	0.09	0.25	0.51	2.17	134.44	0.49	0.243	5.6		[64]
Ruukki-Vihanti (65), FIN (Fe-rich mire precipitates: siderite)		3.30	31.80	0.09	0.43	0.27	0.05	353.33	1.59	0.045	636.0		[64]
Ruukki-Vihanti (67), FIN (Fe-rich mire precipitates: siderite)		2.08	29.10	0.08	0.29	0.31	0.06	363.75	0.94	0.031	485.0		[64]
Ruukki-Vihanti (68), FIN (Fe-rich mire precipitates: siderite)		1.81	37.80	0.17	0.32	0.25	0.04	222.35	1.28	0.021	945.0		[64]
Ruukki-Vihanti (69), FIN (Fe-rich mire precipitates: black amorphous)		1.81	20.90	0.04	0.27	0.47	0.24	522.50	0.57	0.038	87.1		[64]
Ruukki-Vihanti (74), FIN (Fe-rich mire precipitates: black amorphous, siderite)		2.79	19.50	0.03	0.21	0.41	0.13	650.00	0.51	0.062	150.0		[64]
Ruukki-Vihanti (75), FIN (Fe-rich mire precipitates: siderite)		1.56	37.20	0.11	0.28	0.29	0.03	338.18	0.97	0.018	1240.0		[64]
Ruukki-Vihanti (76), FIN (Fe-rich mire precipitates: black amorphous, siderite and vivianite)		7.37	25.90	0.14	0.21	0.42	0.12	185.00	0.50	0.124	215.8		[64]
Peat Kirjaneva, FIN		0.32	4.00	0.02	0.34	0.55	0.63	210.53	0.62	0.035	6.3		[64]
Surface sediments from Roztoka Odrzańska, POL		0.52	2.80	0.17	3.50	0.25	0.95	16.47	14.00	0.081	2.9		This study
Equatorial Pacific (CCFZ) polymetallic nodules, IOM	16.48	0.57	12.50	18.60	2.30	1.60	0.50	0.67	1.44	0.020	25.0	0.357	[73]
Baltic Sea, Słupsk Bank, POL (nodules)	36.76	1.68	13.55	9.75	0.81	1.23	0.04	1.39	0.66	0.054	338.8	0.086	[74]
Szklarka Przygodzicka, POL (solid bog ore)	25.90	4.17	30.61	3.55	0.50	0.05	0.02	8.62	9.26	0.059	1530.5	0.030	[75]
Studzieniec, POL (solid bog ore)	18.32	3.56	38.36	1.42	0.85	0.07	0.08	27.01	12.88	0.040	479.5	0.071	[75]
Wilanów, POL (solid bog ore)	17.83	5.13	43.33	0.60				72.22		0.052			[13]

Table A1. Cont.

Location and Type	SiO ₂	P ₂ O ₅	Fe	Mn	Ca	Mg	S	Fe/Mn	Ca/Mg	P/Fe	Fe/S	(CaO+MgO)/ SiO ₂	Data Source (See References)
			(%)					-	-	-	-	-	
Northern Praga, Warszawa, POL (solid bog ore)	16.41	5.36	49.20	0.36				136.67		0.047			[13]
Brwinów, POL (soft bog ore)	4.49	7.53	45.35	0.87				52.13		0.072			[13]
Tisjoen Lake, NOR (Fe-rich lake nodules)			50.05	1.83				27.35					[25]
Dębe Małe II, POL (soft bog ore)	4.02	7.68	44.16	1.28	2.05	1.52		34.50	1.35	0.076		1.342	[16]
Kolechowice, POL (soft bog ore)	7.88	3.11	33.52	0.17	1.88	0.05		197.18	39.17	0.040		0.344	[16]
Lowland Point (cliff), Lizard, ENG (solid bog ore formed on magmatic rocks)	34.49	0.47	24.05	2.85	0.52	0.78	0.07	8.44	0.67	0.009	343.6	0.059	[76]
Nowosielec, POL (Quaternary bog ore)			42.07										[77]
Wola Chorzewska, POL (Quaternary bog ore)		2.38	26.04	2.04				12.76		0.040			[77]
Cmolas, POL (Quaternary bog ore)		2.41	39.50	1.31				30.15		0.027			[77]
Ruda, POL (Quaternary bog ore)		4.31	31.90	4.52				7.06		0.059			[77]
Biały Bór, POL (Quaternary bog ore)		1.60	33.15	3.18				10.42		0.021			[77]
Lipa, POL (Quaternary bog ore)		1.60	29.32							0.024			[77]
Krownice, POL (Quaternary bog ore)		1.74	27.72	2.62				10.58		0.027			[77]
Ocieka-Zdziary, POL (Quaternary bog ore)		1.52	33.95	4.94				6.87		0.020			[77]
Prażuchy, POL (Quaternary bog ore)			30.04										[77]
Kuźnica-Zakrzyn, POL (Quaternary bog ore)		7.61	40.64	0.81				50.17		0.082			[77]
Annapol, POL (Quaternary bog ore)		4.74	29.53	2.88				10.25		0.070			[77]
Jarantów, POL (Quaternary bog ore)		5.48	36.51	0.35				104.31		0.065			[77]
Stojanów-Modła, POL (Quaternary bog ore)		2.37	24.39	2.22				10.99		0.042			[77]
Sobieski, POL (Quaternary bog ore)		6.75	35.37	2.04				17.34		0.083			[77]
Zajęczki, POL (Quaternary bog ore)		6.73	40.70	1.41				28.87		0.072			[77]
Łęki Godzieskie, POL (Quaternary bog ore)		4.25	24.50	4.87				5.03		0.076			[77]
Grodziec, POL (Quaternary bog ore)		1.86	42.06	0.86				48.91		0.019			[77]
Kolonia Łazińska, POL (Quaternary bog ore)		5.09	34.26	3.87				8.85		0.065			[77]
Gozdów, POL (Quaternary bog ore)		5.58	44.03	1.40				31.45		0.055			[77]
Skrzynno, POL (Quaternary bog ore)		8.80	41.28	1.00				41.28		0.093			[77]
Krzynowłoga Mała, POL (Quaternary bog ore)		2.12	17.57							0.053			[77]

Table A1. Cont.

Location and Type	SiO ₂	P ₂ O ₅	Fe	Mn	Ca	Mg	S	Fe/Mn	Ca/Mg	P/Fe	Fe/S	(CaO+MgO)/ SiO ₂	Data Source (See References)
			(%)					-	-	-	-	-	
Małowidz, POL (Quaternary bog ore)		6.63	33.85							0.085			[77]
Kadzidło, POL (Quaternary bog ore)		2.80	33.44							0.037			[77]
Krobia, POL (Quaternary bog ore)		5.29	34.90							0.066			[77]
Wydmusy, POL (Quaternary bog ore)		3.71	27.40							0.059			[77]
Oberwia, POL (Quaternary bog ore)		4.35	49.84	0.50				99.68		0.038			[77]
Przystań, POL (Quaternary bog ore)		4.38	26.02							0.073			[77]
Łazy, POL (Quaternary bog ore)		3.75	24.93							0.066			[77]
Ruda, POL (Quaternary bog ore)		2.28	32.18							0.031			[77]
Krasny Borek, POL (Quaternary bog ore)		3.97	31.79							0.054			[77]
Krebki, POL (Quaternary bog ore)		3.29	27.33							0.052			[77]
Nowa Ruda, POL (Quaternary bog ore)		5.75	33.27							0.075			[77]
Zabiele, POL (Quaternary bog ore)		4.08	47.82	0.39				122.62		0.037			[77]
Błonie-Miedniewice, POL (Quaternary bog ore)		3.52	34.80	2.43				14.32		0.044			[77]
Garwolin kol. Czarnica, POL (Quaternary bog ore)		2.31	37.97							0.027			[77]
Bramka, POL (Quaternary bog ore)		2.50	33.68							0.032			[77]
Toruń Bobrowniki, POL (Quaternary bog ore)		3.95	41.11	0.22				186.86		0.042			[77]
Szczytno Męcice, POL (Quaternary bog ore)		4.12	37.00	1.22				30.33		0.049			[77]
Lesiny Wielkie, POL (Quaternary bog ore)		2.64	44.00							0.026			[77]
Łuka, POL (Quaternary bog ore)		0.64	35.50							0.008			[77]
Kołodziej Grad, POL (Quaternary bog ore)			28.75										[77]
Myszyniec Wykrot, POL (Quaternary bog ore)		2.65	35.96	0.84				42.81		0.032			[77]
Riga Bay, Baltic Sea, LT (nodules)	24.07	1.65	22.65	10.36	1.54	0.33		2.19	4.67	0.032		0.112	[78]
Finland Bay, Baltic Sea, FIN (nodules)	17.42	2.76	18.96	15.78	1.66	0.60		1.20	2.77	0.063		0.191	[78]
Central Baltic, POL (nodules)	35.33	2.09	16.62	10.80	1.15	0.72		1.54	1.60	0.055		0.079	[78]
residual Jurassic (J2) Fe-rich sands, POL	67.00	0.32	16.20	0.40	0.50	0.10	0.12	40.50	5.00	0.009	135.0	0.013	[79]
Wierzbowia, Bolesławiec, POL (Quaternary bog ore)	28.20	4.58	35.20	2.50				14.08		0.057			[79]
Grabowa, Ostrów Wielkopolski, POL (Quaternary bog ore)	7.20	8.48	48.60	3.40				14.29		0.076			[79]
Zajączki, Ostrów Wielkopolski, POL (Quaternary bog ore)		8.02	47.20	0.60				78.67		0.074			[79]

Table A1. Cont.

Location and Type	SiO ₂	P ₂ O ₅	Fe	Mn	Ca	Mg	S	Fe/Mn	Ca/Mg	P/Fe	Fe/S	(CaO+MgO)/ SiO ₂	Data Source (See References)
			(%)					-	-	-	-	-	
Małowich, Przasnysz, POL (Quaternary bog ore)		6.65	33.80	1.20				28.17		0.086			[79]
Chorzele, Przasnysz, POL (Quaternary bog ore)	10.60	4.28	35.43	0.93				38.10		0.053			[79]
Ziomek, Przasnysz, POL (Quaternary bog ore)	4.60		45.50										[79]
Wólka Kątna, Puławy, POL (Quaternary bog ore)	16.70		28.80										[79]
Cmolasy II, Wisła-San, POL (Quaternary bog ore)	10.50	3.67	42.00	1.30	0.79		1.10	32.31		0.038	38.2	0.105	[79]
Rudawa, Wisła-San, POL (Quaternary bog ore)	33.80	1.15	33.60	1.00				33.60		0.015			[79]
Trzciana, Wisła-San, POL (Quaternary bog ore)	20.00	1.37	33.00	0.90	1.36		2.20	36.67		0.018	15.0	0.095	[79]
Bratkowice, Wisła-San, POL (Quaternary bog ore)	11.30	3.90	34.30	0.30				114.33		0.050			[79]
Jamno, Łódź, POL (Quaternary bog ore)	9.40	7.10	38.50	1.00				38.50		0.080			[79]
Zawady, Łódź, POL (Quaternary bog ore)	15.60	5.27	34.50	1.10				31.36		0.067			[79]
Dylewo, Warszawa, POL (Quaternary bog ore)	4.10	10.54	30.00	0.30	1.57			100.00		0.153		0.536	[79]
Czerwonki Hermanowskie, POL (ochre)	14.10	0.22	45.88	1.40	0.15	0.17		32.77	0.88	0.002		0.035	[80]
Czerwonki Hermanowskie, POL (clayey ochre)	44.76	0.20	22.13	0.85	0.24	0.68		26.04	0.35	0.004		0.033	[80]
Czerwonki Hermanowskie, POL (Fe-nodules)	6.74	0.12	47.38	5.97	0.03	0.01		7.94	3.00	0.001		0.009	[80]
Czerwonki Hermanowskie, POL (Fe-gel)	37.25	5.39	14.10	0.59	1.92	0.19		23.90	10.11	0.167		0.081	[80]
Lorraine I, FRA (Jurassic limonite ore)	8.20	1.37	31.10		9.28	2.61	0.12	3.35	3.56	0.019	259.2	2.113	[81]
Lorraine II, FRA (Jurassic limonite ore)	17.10	1.38	32.10		5.42	1.53	0.28	5.92	3.54	0.019	114.6	0.592	[81]
Maghemite (pure mineral)	0.30		52.15	0.57		5.07						28.054	[82]
Hematite (pure mineral)			69.60	0.67									[82]
Goethite (pure mineral)	0.36		62.67										[82]
Lepidocrocite (pure mineral)			62.84										[82]
Feroxyhyte (pure mineral)			62.85										[82]
Ferrihydrite (pure mineral)			66.21										[82]
Wüstite (pure mineral)	0.14		77.37	0.07									[82]
Siderite (pure mineral)			42.69	0.87	0.07	0.08		609.86	0.88				[82]

Table A1. Cont.

Location and Type	SiO ₂	P ₂ O ₅	Fe	Mn	Ca	Mg	S	Fe/Mn	Ca/Mg	P/Fe	Fe/S	(CaO+MgO)/ SiO ₂	Data Source (See References)
			(%)					-	-	-	-	-	
Vivianite (pure mineral)	0.10	27.17	34.27							0.346			[82]
Metavivianite (pure mineral)		28.40	30.23	3.25	0.36			83.97		0.410			[82]
Strengite (pure mineral)		38.24	30.34							0.550			[82]
Beraunite (pure mineral)		30.17	39.52							0.333			[82]
Phosphosiderite (pure mineral)		38.85	30.97							0.547			[82]
Tomahawk Lake, USA (Fe-rich nodules)	8.02	3.27	54.44	1.14	0.23			236.70		0.026		0.040	[70]
Tomahawk Lake, USA (Mn-rich nodules)	0.27	0.20	0.50	52.88	1.09			0.46		0.174		5.652	[70]
Hershey Bay, USA (Fe-rich nodules)	7.40	2.88	54.86	1.14	0.65			84.40		0.023		0.123	[70]
Hershey Bay, USA (Mn-rich nodules)		0.24	2.05	41.19	2.62			0.78		0.051			[70]
Tomahawk Lake, USA (mean for nodules)	4.15	1.74	27.47	27.01	0.66			118.58		0.100		2.846	[70]
Hershey Bay, USA (mean for nodules)	3.70	1.56	28.46	21.17	1.64			42.59		0.037		0.061	[70]
Green Bay, USA-CAN (freshwater nodules)			27.30										[70]
Northern Lake Michigan, USA-CAN (nodules)			12.40										[70]
Lake Ontario, USA-CAN (nodules)			20.50										[70]
Lake Oneida, USA (nodules)			23.00										[70]
Baltic Sea nodules, POL (type V)	35.30	1.91	12.88	13.69	1.00	1.13		12.88	0.88	0.065		0.093	[83]
Baltic Sea nodules, POL (type T)	57.96	0.96	8.31	2.33	0.44	1.44		18.89	0.31	0.050		0.052	[83]
Baltic Sea nodules, POL (type I)	49.62	1.29	11.29	3.97	0.59	1.42		19.14	0.42	0.050		0.064	[83]
Baltic Sea nodules, POL (type D)	47.62	1.32	10.86	5.22	0.73	1.30		14.88	0.56	0.053		0.067	[83]
Zalew Szczeciński (Szczecin Lagoon), POL (micronodules in lacustrine bog ore)	37.70	3.40	16.44	0.47	4.31	0.20	0.40	3.81	21.55	0.090	41.1	0.169	This study
Dąbie Lake, POL (micronodules in lacustrine bog ore)	7.90	2.64	48.84	3.34	4.12	3.50	1.12	11.85	1.18	0.024	43.6	1.466	This study

References

1. Kotliński, R.; Maciag, Ł.; Zawadzki, D. Potential and Recent Problems of the Possible Polymetallic Sources in the Oceanic Deposits. *Geol. Miner. Resour. World Ocean* **2015**, *40*, 65–80.
2. Taylor, G.; Eggleton, R.A.; Foster, L.D.; Tilley, D.B.; Le Gleuher, M.; Morgan, C.M. Nature of the Weipa Bauxite deposit, northern Australia. *Aust. J. Earth Sci.* **2008**, *55*, 45–70. [\[CrossRef\]](#)
3. Rzepa, G.; Ratajczak, T. *Polskie Rudy Darniowe*; Wydawnictwa AGH: Kraków, Poland, 2011; pp. 1–369.
4. Bricker, O.P.; Newell, W.L.; Simon, N.S. Bog Iron Formation in the Nassawango Creek Watershed, Maryland, USA. In *Geo-Environment: Monitoring and Remediation of the Geological Environment First International Conference on Monitoring, Simulation and Remediation of the Ecological Environment, GEO-ENVIRONMENT 2004*; Martin Duque, J.F., Brebbia, C.A., Godfrey, A.E., Diaz de Teran, J.R., Eds.; USGS: Segovia, Spain, 2004; pp. 13–23. [\[CrossRef\]](#)
5. Thorne, R.L.; Anand, R.R.; Suvorova, A. The formation of fluvio-lacustrine ferruginous pisoliths in the extensive palaeochannels of the Yilgarn Craton, Western Australia. *Sediment. Geol.* **2014**, *313*, 32–44. [\[CrossRef\]](#)
6. Lascelles, D.F. The origin of terrestrial pisoliths and pisolitic iron ore deposits: Raindrops and sheetwash in a semi-arid environment. *Sediment. Geol.* **2016**, *341*, 232–244. [\[CrossRef\]](#)
7. Halbach, P. Mineralogical and geochemical investigations on Finnish lake ores. *Bull. Geol. Soc. Finl.* **1975**, *48*, 33–42. [\[CrossRef\]](#)
8. Szamałek, K. Badania izotopowe pizolitowych kaolinów z okolic Assuanu (Egipt). *Przegląd Geologiczny* **1991**, *461*, 420–422.
9. Szamałek, K.; Barczuk, A.; El Sayed, A.A.Y. Genesis and mineralogy of lateritic kaolin at Aswan area (SW Egypt). *Archivum Mineralogiczne* **1993**, *49*, 81–97.
10. Singh, B.; Gilkes, R.J. Nature and properties of iron rich glaeboles and mottles from some south-west Australian soils. *Geoderma* **1996**, *71*, 95–120. [\[CrossRef\]](#)
11. Mukhopadhyay, J.; Gutzmer, J.; Beukes, N.J.; Bhattacharya, H.N. Geology and Genesis of the Major Banded Iron Formation-Hosted High-Grade Iron Ore Deposits of India. *Rev. Econ. Geol.* **2008**, *15*, 291–316. [\[CrossRef\]](#)
12. Anand, R.R.; Verrall, M. Biological origin of minerals in pisoliths in the Darling Range of Western Australia. *Aust. J. Earth Sci.* **2011**, *58*, 823–833. [\[CrossRef\]](#)
13. Kaczorek, D.; Sommer, M. Micromorphology, chemistry, and mineralogy of bog iron ores from Poland. *Catena* **2003**, *54*, 393–402. [\[CrossRef\]](#)
14. Werońska, A. Wpływ warunków środowiska na powstawanie holocenijskich złóż żelaza. *Gospodarka Surowcami Mineralnymi* **2009**, *25*, 23–36.
15. Jóźwiak, K. Bogs iron ore in the marshy ground areas—E.g. Kampinoski National Park. *Biuletyn Państwowego Instytutu Geologicznego* **2011**, *445*, 237–244.
16. Rzepa, G.; Bajda, T.; Gawęł, A.; Debiec, K.; Drewniak, L. Mineral transformations and textural evolution during roasting of bog iron ores. *J. Therm. Anal. Calorim.* **2016**, *123*, 615–630. [\[CrossRef\]](#)
17. Fedoroff, N.; Courty, M.A.; Guo, Z. Palaeosoils and Relict Soils: A Conceptual Approach. In *Interpretation of Micromorphological Features of Soils and Regoliths*, 2nd ed.; Stoops, G., Marcelino, V., Mees, F., Eds.; Elsevier: Amsterdam, The Netherlands, 2018; pp. 821–862. [\[CrossRef\]](#)
18. Boulangé, B. Les Formations Bauxitiques Latéritiques de Côte d'Ivoire. In *Les Facies, Leur Transformation, Leur Distribution et L'évolution du Model*; Trav. Docum. 175; ORSTOM: Paris, France, 1984; pp. 1–365.
19. Tardy, Y. *Petrology of Laterites and Tropical Soils*; A.A. Balkema Publishers: Rotterdam, The Netherlands, 1997; pp. 1–419.
20. Łydkka, K. *Petrologia Skał Osadowych*; Wydawnictwa Geologiczne: Warszawa, Poland, 1985; pp. 1–286.
21. Horbe, A.M.; Anand, R.R. Bauxite on igneous rocks from Amazonia and Southwestern of Australia: Implication for weathering process. *J. Geochem. Explor.* **2011**, *111*, 1–12. [\[CrossRef\]](#)
22. Nahon, D.B. *Introduction to the Petrology of Soils and Chemical Weathering*; John Wiley & Sons Inc.: New York, NY, USA, 1991; pp. 1–313.
23. Anand, R.R.; Paine, M. Regolith geology of the Yilgarn Craton, Western Australia: Implications for exploration. *Aust. J. Earth Sci.* **2002**, *49*, 3–162. [\[CrossRef\]](#)
24. Ryka, W.; Maliszewska, A. *Słownik Petrograficzny*; Wydawnictwa Geologiczne: Warszawa, Poland, 1991; pp. 1–413.

25. Ljunggren, P. Differential thermal analysis and X-ray examination of Fe and Mn bog ores. *Geologiska Foreningens i Stockholm Forhandlingar* **1955**, *77*, 135–147. [[CrossRef](#)]
26. De Geyter, G.; Vandenberghe, R.G.; Verdonck, L.; Stoops, G. Mineralogy of Holocene bog iron ore in northern Belgium. *Neues Jahrb. Mineral. Abh.* **1985**, *163*, 1–17.
27. Landuydt, C.J. Micromorphology of Iron Minerals from Bog Ores of the Belgian Campine Area. *Dev. Soil Sci.* **1990**, *19*, 289–294. [[CrossRef](#)]
28. Cornell, R.M.; Schwertmann, U. *The Iron Oxides. Structure, Properties, Reactions, Occurrences and Uses*; VCH: Weinheim, Germany, 1998; pp. 1–664. [[CrossRef](#)]
29. Stoops, G. SEM and Light Microscopic Observations of Minerals in Bog-Ores of the Belgian Campine. *Dev. Soil Sci.* **1983**, *12*, 179–186. [[CrossRef](#)]
30. Mermut, A.R.; Dasog, G.S. Nature and Micromorphology of Carbonate Glaebules in Some Vertisols of India. *Soil Sci. Soc. Am. J.* **1986**, *50*, 382–391. [[CrossRef](#)]
31. Gallaher, R.N.; Perkins, H.F.; Tan, K.H. Chemical and mineralogical changes in glaebules and enclosing soil with depth in a plinthic soil. *Soil Sci.* **1974**, *117*, 336–342. [[CrossRef](#)]
32. Piotrowski, S. Geochemical characteristics of bottom sediments in the Odra River estuary—Roztoka Odrzańska (north-west Poland). *Geol. Q.* **2004**, *48*, 61–76.
33. Copernicus Sentinel Data 2016 & 2017. EOX IT Services GmbH. Available online: <https://sentinel.esa.int> (accessed on 1 May 2019).
34. Buchholz, W.; Kreft, A.; Parzonka, W.; Coufal, R.; Meyer, Z. Warunki hydrologiczne estuarium Odry. In *Regionalne Problemy Gospodarki Wodnej i Hydrotechniki*; Wydawnictwo Uczelniane PS: Szczecin, Poland, 2004; pp. 11–20.
35. Piotrowski, A. *Objaśnienia do Szczegółowej Mapy Geologicznej Polski 1:50,000, Arkusz Police (190)*; Wyd. Państwowego Instytutu Geologicznego: Warszawa, Poland, 1982; pp. 1–82.
36. Malinowski, R.; Niedźwiecki, E.; Kowalski, W.A.; Protasowicki, M. Charakterystyka wybranych elementów środowiska przyrodniczego Wyspy Chełminek. Cz. I. Różnicowanie się cech morfologicznych i właściwości gleb powstających z piaszczystych osadów dennych w wyniku ich zalesienia na wyspie Chełminek. *Folia Pomer. Univ. Technol. Stetin. Ser. Agric. Aliment. Pisc. Zootech* **2012**, *300*, 73–82.
37. Kowalewska-Kalkowska, H. Rola Wezbrań Sztormowych w Kształtowaniu Ustroju Wodnego Układu Dolnej Odry i Zalewu Szczecińskiego; Wydawnictwo Naukowe US: Szczecin, Poland, 2012; pp. 1–258.
38. Borówka, R. Krajobrazy Zalewu Szczecińskiego i jego otoczenia. *Prace Komisji Paleogeografii Czwartorzędu Polskiej Akademii Umiejętności* **2003**, *1*, 89–91.
39. Duda, T. Sedymentacja osadów fluwalnych w Dolinie Dolnej Odry rozwijającej się pod wpływem długotrwałego wzrostu poziomu morza. In *Rozprawy i Studia (945)871*; Wydawnictwo Naukowe US: Szczecin, Poland, 2013; pp. 1–156.
40. Poleszczuk, G.; Piesik, Z. On differences in chemical composition occurring between surface and near bottom water in the Szczecin Lagoon. *Balt. Coast. Zone* **2000**, *4*, 27–43.
41. Landsberg-Ucziwek, M.; Złoczorska, I.; Kordas, A.; Wierchowaska, E.; Mazur-Chrzanowska, B.; Sroka, E.; Konon-Szatowska, H.; Gajdecki, A. *Ocena Jakości wód Powierzchniowych w Województwie Zachodniopomorskim za 2015 Rok*; Archiwum WIOŚ w Szczecinie: Szczecin, Poland, 2016.
42. Nałęcz, T. *Geochemical Atlas of Szczecin Agglomeration, Part II*; Ekologicznej, S.A., Ed.; Wydawnictwo Kartograficzne Polskiej Agencji: Warszawa, Poland, 1998; pp. 1–16.
43. Romanowska-Duda, Z. Metale ciężkie jako specyficzne zanieczyszczenia środowiska wodnego. *Acta Innov.* **2015**, *15*, 1–18.
44. Lis, J.; Pasieczna, A. *Geochemical Atlas of Szczecin Agglomeration, Part I*; Ekologicznej, S.A., Ed.; Wydawnictwo Kartograficzne Polskiej Agencji: Warszawa, Poland, 1998; pp. 1–18.
45. Borówka, R.; Skowronek, A.; Osadczuk, A.; Witkowski, A.; Maciag, Ł.; Tomkowiak, J.; Bieniek, B.; Kosińska, B. Litologia i geochemia osadów wschodniej części Zalewu Szczecińskiego (Zalew Wielki). In *Budowa Geologiczna Południowego Bałtyku i Pomorza Środkowego Oraz Aktualne Problemy Geologii Morza w Perspektywie Polskich Badań Oceanicznych, Proceedings of the 85 Zjazd Naukowy Polskiego Towarzystwa Geologicznego, Koszalin, Poland, 18–21 September 2017*; Państwowy Instytut Geologiczny-Państwowy Instytut Badawczy PGI-PIB: Warszawa, Poland, 2017; pp. 43–50.
46. Piotrowski, S. Zawartość metali ciężkich (Cu, Zn, Pb, Co, Cd, Hg) w wybranych elementach ekosystemu estuarium Odry. *Przegląd Geologiczny* **2007**, *55*, 193–197.

47. Lithogenetic Map of Poland. Available online: www.geolog.gov.pgi.pl (accessed on 1 June 2019).
48. Grazulis, S.; Chateigner, D.; Downs, R.T.; Yokochi, A.T.; Quiros, M.; Lutterotti, L.; Manakova, E.; Butkus, J.; Moeck, P.; Le Bail, A. Crystallography Open Database—An open-access collection of crystal structures. *J. Appl. Cryst.* **2009**, *42*, 726–729. [[CrossRef](#)]
49. Alvarez, M.; Sileo, E.E.; Rueda, E.H. Structure and reactivity of synthetic Co-substituted goethites. *Am. Mineral.* **2008**, *93*, 584–590. [[CrossRef](#)]
50. Gualtieri, A.; Venturelli, P. In situ study of the goethite-hematite phase transformation by real time synchrotron powder diffraction. *Am. Mineral.* **1999**, *84*, 895–904. [[CrossRef](#)]
51. Patrat, G.; de Bergevin, F.; Pernet, M.; Joubert, J.C. Structure locale de δ -FeOOH. *Acta Crystallogr. Sect. B Struct. Sci.* **1983**, *39*, 165–170. [[CrossRef](#)]
52. Goldsztaub, M. Etude de quelques derives de l'oxyde ferrique (FeOOH, FeO₂Na, FeOCl) determination de leurs structures. *Bulletin de la Societe Francaise de Mineralogie* **1935**, *58*, 6.
53. Jansen, E.; Kyek, A.; Schafer, W.; Schwertmann, U. The structure of six-line ferrihydrite. *Appl. Phys. A* **2002**, *74*, 1004–1006. [[CrossRef](#)]
54. Zhang, J.; Guyot, F. Thermal equation of iron and Fe_{0.91}Si_{0.09}. *Phys. Chem. Mineral.* **1999**, *26*, 206–211. [[CrossRef](#)]
55. Mori, H.; Ito, T. The structure of vivianite and symplectite. *Acta Crystallogr.* **1950**, *3*, 1–6. [[CrossRef](#)]
56. Chukanov, N.V.; Scholz, R.; Aksenov, S.M.; Rastsvetaeva, R.K.; Pekov, I.V.; Belakovskiy, D.I.; Krambrock, K.; Paniago, R.M.; Righi, A.; Martins, R.F.; et al. Metavivianite, Fe²⁺Fe³⁺₂(PO₄)₂(OH)₂·6H₂O: New data and formula revision. *Mineral. Mag.* **2012**, *76*, 725–741. [[CrossRef](#)]
57. Lavina, B.; Dera, P.; Downs, R.T.; Yang, W.; Sinogeikin, S.; Meng, Y.; Shen, G.; Schiferl, D. Structure of siderite FeCO₃ to 56 GPa and hysteresis of its spin-pairing transition. *Phys. Rev. B* **2010**, *82*, 110–118. [[CrossRef](#)]
58. Gualtieri, A.F. Accuracy of XRPD QPA using the combined Rietveld-RIR method. *J. Appl. Crystallogr.* **2000**, *33*, 267–278. [[CrossRef](#)]
59. Gournis, D.; Lappas, A.; Karakassides, M.A.; Tobbens, D.; Moukarika, A. A neutron diffraction study of alkali cation migration in montmorillonites. *Phys. Chem. Mineral.* **2008**, *35*, 49–58. [[CrossRef](#)]
60. Nickel, E.H. New data on woodwardite. *Mineral. Mag.* **1976**, *43*, 644–647. [[CrossRef](#)]
61. Witzke, T.; Raade, G. Zincwoodwardite, [Zn_{1-x}Al_x(OH)₂](SO₄)_{x/2}(H₂O)_n], a new mineral of the hydrotalcite group. *Neues Jahrbuch für Mineralogie Monatshefte* **2000**, *10*, 455–465.
62. Effenberger, H.; Mereiter, K.; Zemmann, J. Crystal structure refinements of magnesite, calcite, rhodochrosite, siderite, smithonite, and dolomite, with discussion of some aspects of the stereochemistry of calcite type carbonates. *Zeitschrift für Kristallographie, Kristallgeometrie, Kristallphysik, Kristallchemie* **1981**, *156*, 233–243.
63. Fjellvag, H.; Hauback, B.C.; Vogt, T.; Stolen, S. Monoclinic nearly stoichiometric wüstite at low temperatures. *Am. Mineral.* **2002**, *87*, 347–349. [[CrossRef](#)]
64. Virtanen, K. Geological control of iron and phosphorous precipitates in mires of the Ruukki-Vihanti area, Central Finland. *Bull. Geol. Surv. Finl.* **1994**, *375*, 1–69.
65. Postma, D. Formation of siderite and vivianite and the porewater composition of a recent bog sediment in Denmark. *Chem. Geol.* **1981**, *31*, 225–244. [[CrossRef](#)]
66. Postma, D. Pyrite and siderite formation in brackish and freshwater swamp sediments. *Am. J. Sci.* **1982**, *282*, 1151–1183. [[CrossRef](#)]
67. Wang, J.; Chen, J.; Guo, J.; Sun, Q.; Yang, H. Combined Fe/P and Fe/S ratios as a practicable index for estimating the release potential of internal-P in freshwater sediment. *Environ. Sci. Pollut. Res.* **2018**, *25*, 10740–10751. [[CrossRef](#)]
68. Jensen, H.S.; Kristensen, P.; Jeppesen, E.; Skytte, A. Iron:phosphorus ratio in surface sediment as an indicator of phosphate release from aerobic sediments in shallow lakes. *Hydrobiologia* **1992**, *235*, 731–743. [[CrossRef](#)]
69. Migaszewski, Z.M.; Gałuszka, A. *Geochemia Środowiska*; Wydawnictwa Naukowe PWN: Warszawa, Poland, 2007; pp. 1–574.
70. Jones, B.F.; Bowser, C.J. The mineralogy and related chemistry of lake sediments. In *Lakes, Chemistry, Geology, Physics*; Lerman, A., Ed.; Springer: New York, NY, USA, 1978; pp. 179–236.
71. Mozley, P.S. The internal structure of carbonate concretions in mudrocks: A critical evaluation of the conventional concentric model of concretion growth. *Sedim. Geol.* **1996**, *103*, 85–91. [[CrossRef](#)]
72. Clarke, J.D.A.; Chenoweth, L. Classification, genesis and evolution of ferruginous surface grains. *AGSO J. Aust. Geol. Geophys.* **1996**, *16*, 213–221.

73. Depowski, S.; Kotliński, R.; Rühle, E.; Szamałek, K. *Surowce Mineralne Mórz i Oceanów*; Wydawnictwo Naukowe SCHOLAR: Warszawa, Poland, 1998; pp. 1–384.
74. Szamałek, K.; Uścińowicz, S.; Zglinicki, K. Rare earth elements in Fe-Mn nodules from southern Baltic Sea—A preliminary study. *Biuletyn Państwowego Instytutu Geologicznego* **2018**, *472*, 199–212. [[CrossRef](#)]
75. Kraczkowska, I.; Ratajczak, T.; Rzepa, G. Skład mineralny oraz właściwości fizykomechaniczne kawałkowych odmian rud darniowych stosowanych w historycznym budownictwie na ziemiach polskich. *Przegląd Geologiczny* **2001**, *49*, 1147–1156.
76. Scott, P.W.; Ealey, P.J.; Rollinson, G.K. Bog iron ore from Lowland Point, St Keverne, Lizard, Cornwall. *Geosci. South-West Engl.* **2011**, *12*, 260–268.
77. Kociszewska-Musiał, G. *Surowce Mineralne Czwartorzędu*; Wydawnictwa Geologiczne: Warszawa, Poland, 1988; pp. 1–280.
78. Warendow, I.; Błaszczyszyn, A. Konkrecje manganowe w dnie Morza Bałtyckiego. In *Geologia Morza Bałtyckiego*; Gudelis, W.K., Jemielianow, J.M., Eds.; Wydawnictwa Geologiczne: Warszawa, Poland, 1982; pp. 307–345.
79. Białaczewski, A. Rudy darniowe. In *Budowa Geologiczna Polski, Złoża Surowców Mineralnych*; Osika, R., Ed.; Wydawnictwa Geologiczne: Warszawa, Poland, 2007; Volume 6, pp. 278–282.
80. Kotlarczyk, J.; Ratajczak, T. *Ochra Karpacka z Czerwonek Hermanowskich koło Tyczyna*; Wydawnictwo IGSMiE PAN: Kraków, Poland, 2002; pp. 1–120.
81. Wyderko-Delekta, M.; Bolewski, A. *Mineralogia Spieków i Grudek Rudnych*; Wydawnictwa AGH: Kraków, Poland, 1995; pp. 1–280.
82. Mineral Data Publishing, Version I. Available online: www.webmineral.com (accessed on 1 June 2019).
83. Zglinicki, K.; Szamałek, K.; Uścińowicz, S.; Damrat, M.; Szeffler, K.; Nowak, J.; Zhamoida, V.; Krek, A.; Bubnova, E. Metale w konkrecjach Fe-Mn z polskiego sektora Morza Bałtyckiego. In Proceedings of the II Konferencja Naukowa Polskich Badaczy Morza, Gdynia, Poland, 24–25 September 2019. [[CrossRef](#)]



© 2019 by the authors. Licensee MDPI, Basel, Switzerland. This article is an open access article distributed under the terms and conditions of the Creative Commons Attribution (CC BY) license (<http://creativecommons.org/licenses/by/4.0/>).